Optimization and Evaluation of Drone Operational Parameters for Enhanced Spray Efficiency in a Peach Tree Orchard

by

Lucas Barion de Oliveira

A thesis submitted to the Graduate Faculty of
Auburn University
in partial fulfillment of the
requirements for the Degree of
Master of Science

Auburn, Alabama
August 9, 2025

Keywords: drone operational parameters, pesticide application, spray efficiency

Approved by

Andre Luiz Biscaia Ribeiro da Silva, Chair, Assistant Professor of Horticulture
Camila Rodrigues, Assistant Professor of Horticulture
Wheeler Foshee, Professor of Horticulture
Clive Bock, Research Plant Pathologist, USDA

Abstract

This study evaluated the effectiveness of drone-based pesticide application in fruit orchards using a DJI Agras T40. Two experiments were conducted: one in a simulated canopy and another in a peach orchard, assessing the effects of operation mode, application volume, flight height, and droplet size on spray coverage, droplet density, droplet diameter, and droplet size uniformity. Three drone operational modes (standard, fruit tree, and spinning) were tested. In the simulated canopy, the spinning mode achieved the highest coverage (20.81%) and droplet density (172.44 drops/cm^2), while the standard mode offered the most uniform distribution. In the orchard, the fruit tree mode achieved the highest spray coverage (6.55%) and droplet density (90.09 drops/cm^2). The conventional air-blast sprayer provided greater coverage (58.77%) and droplet density (193.11 drops/cm^2), the drone treatments however, demonstrated efficient canopy penetration and reduced chemical use, especially in targeted applications. These findings support the potential of optimized drone spraying as a sustainable and efficient alternative for precision agriculture and informed future design improvements for orchard pest management.

Acknowledgments

First, I want to thank God for giving me the strength, patience, and guidance to make it through this journey. I truly wouldn’t be here without His presence in my life. I would like to express my gratitude to my amazing wife, Jessica dos Santos Pizzo, thank you for your endless support, love, and patience. You’ve been my rock during every challenging moment. I couldn’t have done this without you. To my family, thank you for always being there with encouragement, prayers, and belief in me. Your support brought me here.

I’m incredibly grateful to my advisor, Dr. Andre Da Silva, for his mentorship, encouragement, and for always pushing me to grow as a researcher and professional. Thank you for your time, wisdom, and support. To my committee members, Dr. Camila Rodrigues, Dr. Wheeler Foshee, and Dr. Clive Bock, thank you for your valuable feedback, support, and time. To my colleagues and friends, thank you for your help, motivation, and all the good memories. Lastly, I want to thank the Department of Horticulture and Auburn University for providing the opportunities, resources, and support that made this work possible.

Table of Contents

List of Tables

List of Figures

Chapter I

Literature Review

1. FRUIT TREE PRODUCTION - OVERVIEW

A fruit tree is defined as a tree that produces edible fruits, nuts, or beans (Santosa et al., 2021). These trees exhibit considerable diversity in size, shape, and fruit type (Muthuri et al., 2023). Common examples include apples, pear, pecan, hazelnut, and peach trees (Hoying, 2017; Muthuri et al., 2023; Perez et al., 2017).

Fruit tree production plays a vital role in the United States (U.S.) agriculture industry. In 2017, the total value of fruit and vegetable production was $48.2 billion, representing 25% of the national crop production (Huang et al., 2022). Specifically, sales from fruits, tree nuts, and berries reached $28.6 billion, exceeding the market value of hogs and pigs, which was $26.3 billion (Fruit, Tree Nut, and Berry Production, 2017). By 2022, U.S. sales of fruit, tree nut, and berry had increased to $34.2 billion, marking a 20% rise compared to 2017 (USDA, 2022).

Almonds currently lead U.S. fruit production, with over 1.6 million bearing acres, accounting for half of the country's tree nut production—nearly all of which is cultivated in California (USDA, 2022). Grapes rank second, covering 1.1 million bearing acres and representing 52% of non-citrus fruit acreage, with almost 80% of production concentrated in California. Pecans constitute 18% of total tree nut acreage, covering more than 600,000 bearing acres. California remains the top state for fruit, tree nut, and berry sales, totaling over $23 billion, followed by Washington ($3.7 billion) and Florida ($1.4 billion) (USDA, 2022).

Sustaining consistent fruit production requires the effective use of pesticides. However, concerns regarding chemical contamination posing risks to consumers health and the environment (Carvalho, 2017; Schreinemachers et al., 2020; Tudi et al., 2021). Additionally, the use of these chemicals can be costly. According to the United States Department of Agriculture (USDA, 2022), in 2022, farms specializing in fruit, tree nut, and berry production had a total production cost of $29.9 billion, with chemicals expenses ranking as the third-largest cost category, accounting for nearly 10% of the total production costs. These challenges highlight the need for safer, more efficient, and precise pesticide application methods.

1.1. Peach production

Peach (*Prunus persica* (L.) Batsch) is one of the most cultivated fruit crops in the world (Manganaris et al., 2022). According to the USDA (2024) China leads the world peach production, followed by the European Union (EU), Turkey, and the U.S. (Protzman, 2023). Although global peach production increased from 19.6 million tons in 2013/14 to 24.2 million tons in 2022/23, this growth masks an overall decline in several key countries, including the EU and the U.S. (Protzman, 2023).

In the U.S. peach production has decreased significantly over the past decade, declining from 930,000 tons to 650,000 tons—a reduction of more than 30% (USDA, 2023). This decline has occurred across nearly all production states, with California, which accounts for 80% of total U.S. production, experiencing the sharpest drop. Since 2013/14, California's combined production of peaches and nectarines has decreased by more than 200,000 tons, with Clingstone peaches, primarily used for processing, experiencing a 43% decline over the same period (Protzman, 2023). U.S. per capita peach consumption has also decreased, from 3.0 kg in 1980 to 0.96 kg in 2019 (Anthony & Minas, 2022).

One of the primary factors contributing to the decline in peach production is the susceptibility of peaches to various pests, fungal infections, and bacterial diseases that can significantly reduce fruit yield and quality. In 2018, major peach diseases in Georgia alone resulted in over $5 million in total costs, with $3.9 million spent specifically on disease control (Brannen, 2018). Brown rot, caused by *Monilinia fructicola,* is one of the most economically harmful fungal diseases for peach worldwide (Luo et al., 2022) and accounted for the highest control costs, totaling $2 million. Meanwhile, Armillaria root rot resulted in economic losses of nearly $500,000 (Brannen, 2018). Peach Scab, caused by *Venturia carpophila*, is particularly prevalent in the southeastern U.S. (Schnabel & Brannen, 2022), with control costs reaching $1.5 million (Brannen, 2018). Additionally, phony peach disease, caused by the bacterium *Xylella fastidiosa*, had a significant economic impact on peach production, contributing to nearly $400,000 in losses (Brannen, 2018).

2. PESTICIDE USE

Pesticides are chemicals widely used in agriculture to control pests, such as rodents, insects, fungi, and weeds (EPA, 2025). These include fungicides, herbicides, insecticides, and disinfectants, each designed to target specific pests (EPA, 2024). In agricultural development, pesticides have become essential tools for plant protection and enhancing crop yields (Sharma et al., 2019). Approximately 78% of fruit production is lost due to pest and diseases, highlighting the need for effective pest management through the use of pesticides to combat these threats and increase crop production (Luo et al., 2022; Sharma et al., 2019; Tudi et al., 2021).

As the global population increases, the demand for pesticide use also grows. In the 1950s, around 0.2 million tons of pesticides were used worldwide in agriculture. By 2022, the amount had risen to 3.7 million tons (Carvalho, 2017; FAOSTAT, 2022). The top five pesticide-consuming countries are the U.S., Brazil, China, Indonesia, and Argentina (FAOSTAT, 2022).

Despite the significant increase in pesticide usage, only a small fraction of these chemicals effectively reaches their targets. A significant amount enters the environment, contributing to pollution, health risks, and higher costs for growers (Maggi et al., 2023; Tudi et al., 2021). According to a study from the University of Sydney, approximately 80% of applied pesticides degrade into byproducts in the soil and around 70,000 tons of pesticide residue enter aquifers annually (Maggi et al., 2023).

Studies have highlighted the widespread overuse of pesticides in agriculture. For example, Schreinemachers et al. (2020) evaluated pesticide use among 1,000 farmers in South Asia, specifically in Cambodia, Laos, and Vietnam. Their finding revealed that pesticide overuse is prevalent, with 100% of farmers in Vietnam, 73% in Cambodia, and 59% in Laos exceeding the recommended pesticide application levels. Cai et al. (2021) evaluated pesticide overuse in apple production, focusing on farmers' attitudes toward risk. Their study in Shaanxi and Shandong provinces, China, identified that more risk-averse farmers tend to overuse pesticides. Larger orchards and older apple trees also contributed to increased pesticide applications. This highlights the need for sustainable and effective pest management practices to minimize chemical pesticide use, such as organic crop production (Durham & Mizik, 2021; Kumhar et al., 2022; Kuosmanen et al., 2021), crop diversity (Thomine et al., 2022), information propagation (Zhao et al., 2020), and low-volume spraying (Arakawa & Kamio, 2023).

Studies have demonstrated opportunities to reduce pesticide overuse through low-volume spray application methods (Arakawa & Kamio, 2023; Jiang et al., 2022; Nan et al., 2023). Miguez et al. (2019) used a Tree Row Volume (TRV) approach to determine the volume of vegetation per unit area of peach and lemon trees. Initial tests demonstrated a reduction of product of 33% in lemon and 55% in peaches, while spray quality was still maintained.

Berger-Neto et al. (2017) conducted two to evaluate the effectiveness of fluazinam and procymidone fungicides applied at spray volumes of 100 and 200 L/ha, using three different nozzle types, including a hollow cone nozzle, a pre-orifice flat dan nozzle, an induction air flat fan nozzle and a standard flat fan nozzle, to control white mold in soybeans. Their results indicated that spray volume did not significantly impact white mold control. However, air induction flat-fan nozzles were more effective in reducing both white mold incidence and sclerotia production. In addition, procymidone was more effective than fluazinam in reducing sclerotia production. No differences in yield were observed among the studied factors, indicating that nozzle type, rather than spray volume, is critical for effective white mold control.

3. METHODS OF PESTICIDE APPLICATION IN FRUIT TREES

Spraying fruit trees can be a challenge as many trees have tall canopies and dense branches. In addition, the difference in the tree structure at different growth stages complicates the spraying process. Different methods can be used to apply pesticides in fruit tree, including conventional techniques, such as air-blast sprayers, tunnel sprayers and tower sprayers (Mahmud et al., 2021), as well as emerging technologies such as variable-rate sprayers (Wandkar et al., 2018), unmanned ground vehicles (Jiang et al., 2022) and unmanned aerial vehicle (UAV) (Li et al., 2021; Martinez-Guanter et al., 2020). Each of these methods presents unique advantages and disadvantages. To address the diverse needs of fruit trees cultures at different growth stages, research has focused on developing new technologies specifically designed for orchards spraying (Wei, Li, et al., 2023).

3.1. Conventional methods for pesticide application in fruit trees

Conventional spraying techniques, including the use of air-blast sprayers, tunnel sprayers, tower sprayers, cannon sprayers, and custom-made or modified sprayers, are widely employed in fruit orchards. Among these, air-blast sprayers are the most commonly used (Mahmud et al., 2021).

Air-blast sprayers (Figure 1) are machines equipped with a fan at the back that draws in air and directs it upward, carrying a solution from the tank and dispersing it onto the tree canopy

(Mahmud et al., 2021). Air-blast sprayers are favored for their effectiveness in reaching various parts of the tree canopy, achieving a pesticide utilization rate of 30–40% (Hu et al., 2022).

Figure 1. Air blast sprayers used in fruit orchard.

However, air-blast sprayers face several challenges. Conventional axial-fan air-blast sprayers apply pesticides at a constant rate, often resulting in excessive application, leading to increased costs and environmental contamination (Wei, Xue, et al., 2023). Moreover, these sprayers may be less effective on taller trees. For instance, studies have shown that even the most powerful air-blast sprayers are effective in controlling diseases in trees up to only approximately

12.5 m in height, but their efficacy diminishes on trees taller than this, with disease approaching levels seen in untreated trees (Bock & Hotchkiss, 2020).

3.2. UAV technology for pesticide application in fruit trees

UAV, commonly known as drones, have emerged as a promising technology for pesticide application in orchards (Lopes et al., 2023). Despite their compact size, drone sprayers incorporate all essential components found in larger ground-based and conventional aerial sprayers, including tank, pump, pressure gauge, hoses, filters, nozzles, and a flow meter (Ozkan, 2024). In addition to these components, all drone sprayers are equipped with a Global Navigation Satellite System (GNSS) receiver for precise navigation and multiple sensors for collision avoidance. These drones are operated via wireless remote control, allowing for efficient and flexible spraying operations (Ozkan, 2024).

Drones can be classified based on their configuration and number of rotors (Mohsan et al., 2023). Single-rotor helicopters (Figure 2A) feature a large primary rotor and a smaller tail rotor for stability and control. Multi-rotor drones (Figure 2B-C), including quadcopters, hexacopters, and octocopters, use four, six, or eight rotors, respectively, for propulsion and lift (Benos et al., 2023). In contrast, fixed-wing drones (Figure 2D) have wing designs similar to gliders, which allows for longer flight durations and different aerodynamic functions (Mogili & Deepak, 2018).

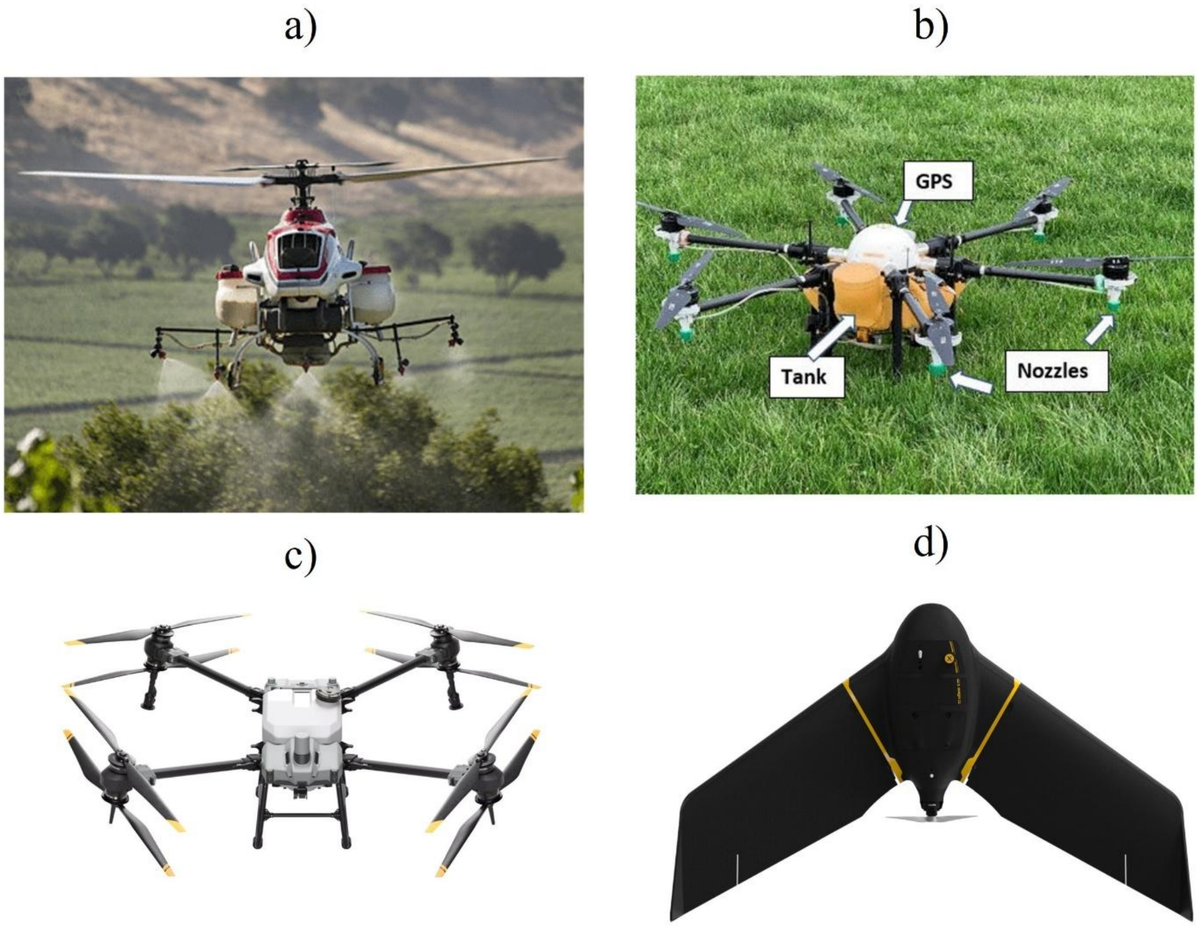

Figure 2. Drone configurations for pesticide application: a) Single-rotor helicopter drone, b) Multi-rotor drone with no boom nozzle configuration, c) Multi-rotor drone with a boom-mounted nozzle configuration, and d) Fixed-wing drone (*AgEagle*, 2025; Ozkan, 2024)

In multi-rotor drones, nozzles are typically positioned below the rotors to maximize spray swath width as the drone moves across the crop canopy (Ozkan, 2024). This arrangement leverages rotor-generated airflow to enhance canopy penetration and improve pesticide deposition (Tang et al., 2023)). However, some multi-rotor platforms (Figure 2C) utilize a boom-mounted nozzle system, in which nozzles are arranged along a horizontal structure beneath the drone (P. Chen et al., 2022). Multi-rotor drones with boom-mounted nozzles have demonstrated poorer spray coverage compared to boomless configurations, which position the nozzles directly under the rotors. Additionally, boom-mounted systems tend to have a higher drift potential and an increased likelihood of vortex formation near the boom edges, which can negatively affect spray uniformity (Ozkan, 2024). Multi-rotor drones are commonly used in precision agriculture due to their ability to cover small areas in a few flights and operate at lower speeds, making them highly maneuverable and cost-effective (Tsouros et al., 2019).

One of the significant advantages of drones is their vertical takeoff and landing capability, which allows them to operate in constrained spaces with minimal need for a landing area, unlike many fixed-wings drones, that require large, unobstructed spaces for takeoff and landing (van der Merwe et al., 2020). Additionally, drones can fly above the tree canopy, providing enhanced coverage compared to conventional ground-based sprayers, which are often limited by tree height (Mahmud et al., 2023). Drones are also effective in orchards with uneven terrain or slopes that may be inaccessible to tractor-mounted sprayers. In contrast to conventional sprayers, drones only require a flat surface for takeoff and landing (van Veelen et al., 2023). Moreover, drones' low-volume capacity contributes to a reduction in the overall amount of chemicals applied to crops, leading to more sustainable pesticide use (Shan et al., 2024a).

Arakawa & Kamio (2023) investigated the efficacy of different insecticides applied to chestnut trees using various UAVs, including a P20 (XAG), TDS-AG10 (TDS), T20K (Kubota), Agras T10 (Shenzhen DJI Innovation Technology), and T30 (Shenzhen DJI Innovation Technology). Their study compared drone applications with conventional air-blast sprayers and high-pressure sprayers, finding that drone spraying achieved 84% control efficacy, compared to 78% for conventional methods. The authors concluded that drones represent a promising technology for insect control, offering significant benefits in reducing labor costs and minimizing health risks.

In a different study, Li et al. (2021) compared spray deposition and canopy penetration between drone technology and conventional ground-based spraying in almond orchards. While conventional methods provided higher overall spray coverage, drones achieved better coverage of the upper canopy when using a higher spray volume (93.5 L/ha) compared to a lower volume (46.8 L/ha). This highlights the importance of adhering to recommended spray volumes for effective pest control.

Sassu et al. (2024) investigated the impact of flight parameters, such as position, height, and speed, on the distribution of plant protection products (PPP) applied by drones in vineyards. They found that optimal results were achieved by flying 2 m above the ground, positioning the drone in the inter-row area, and placing nozzles directly above the canopy. This setup improved spray penetration into the lower canopy, reduced off-target dispersion, and enhanced overall spraying efficiency. While flight speed had minimal impact, increased propeller rotation speed enhanced droplet penetration. The study highlights drone's potential for efficient spraying but emphasized the need for further research into their environmental impact and effectiveness.

Several factors influence treatment outcomes when using drones for spraying, including spray and flight settings (e.g., volume, flight height, droplet size, and speed), payload capacity, weather conditions (such as wind direction and speed), flight range, and environmental factors such as ground leakage (H. Chen et al., 2021; Sassu et al., 2024). Another factor influencing drone spray efficiency is the downwash, a downward airflow generated by rotor thrust. This airflow influences spray behavior by propelling droplets deeper into the canopy, thereby enhancing deposition uniformity (P. Chen et al., 2022). However, in some cases, rotor-induced airflow can also push airborne droplets outward, increasing off-target drift and reducing application efficiency (Delavarpour et al., 2023). The magnitude of downwash varies depending on several factors, including drone payload weight, flight speed, and altitude, all of which must be optimized to achieve effective pesticide application (J. Wang et al., 2018; Zhan et al., 2022). All these parameters directly impact spray coverage, droplet density, droplet size, and overall spray quality, ultimately influencing disease control efficacy (Li et al., 2021). Therefore, understanding the impact of different flight and spray settings is critical for optimizing drone spraying effectiveness.

4. DROPLET DEPOSITION

Effective droplet deposition is a critical factor in pesticide application, as it directly influences pest control efficacy (S. Guo et al., 2019; Muhammad et al., 2019; Srinivasarao et al., 2021). For optimal performance, spray droplets must reach and adhere to the target surface, ensuring sufficient coverage and absorption (Song et al., 2022). However, a significant proportion of sprayed droplets often miss their target, leading to pesticide wastage, reduced effectiveness, and potential environmental contamination (S. Guo et al., 2019). Therefore, evaluating spray characteristics, such as coverage, droplet size, droplet density, and spray uniformity, is essential to optimize pesticide applications (Srinivasarao et al., 2021).

Droplet size plays a vital role in determining pesticide application efficacy. Small droplets are more susceptible to drift and evaporation, which can decrease spray effectiveness and increase the risk of environmental contamination (Privitera et al., 2023). However, they also exhibit better canopy penetration, enhancing overall coverage and deposition uniformity (Nogueira Martins et al., 2021; Nuyttens et al., 2007). In contrast, larger droplets are less susceptible to wind drift but may result in excessive runoff and decreased target coverage (Srinivasarao et al., 2021).

The impact of droplet size and density on spray effectiveness also varies depending on the mode of action of the applied pesticide. Systemic pesticides do not require complete and uniform surface coverage, as larger droplets facilitate absorption and translocation within plant tissues

(Hanna et al., 2009; Privitera et al., 2023). These pesticides are absorbed through roots or leaf surfaces and subsequently transported throughout the plant (Privitera et al., 2023; Srinivasarao et al., 2021). In contrast, contact pesticides require direct exposure to the target surface and demand thorough coverage, making smaller droplets more effective for achieving sufficient leaf surface deposition (Privitera et al., 2023).

The most used parameter for characterizing droplet size is the volumetric diameter (Dv0.5), also known as the volume median diameter (VMD) (Privitera et al., 2023). The VMD represents the droplet diameter at which 50% of the sprayed solution consists of smaller droplets, while the other 50% consists of larger droplets (Srinivasarao et al., 2021).

To standardize droplet classification, the American Society of Agricultural and Biological Engineers (ASABE) Standard 572 categorizes droplets based on their VMD size (Table 1).

Table 1. Droplet classification based on volume median diameter (VMD).

Droplet category	**VMD range (µm)**
Extremely fine	<60
Very fine	61-105
Fine	106-235
Medium	236-340
Coarse	341-403
Very coarse	404-502
Extremely coarse	503-665
Ultra coarse	>665

In addition to the VMD, two other key metrics are commonly used for droplet characterization: Dv0.1 and Dv0.9. The Dv0.1 indicates the droplet diameter at which 10% of the total spray volume consists of droplets equal to or smaller than this value. A lower Dv0.1 value increases the potential for drift. The Dv0.9 represents the droplet diameter at which 90% of the total spray volume consists of droplets equal to or smaller than this value. A higher Dv0.9 suggests that a significant proportion of the spray volume comprises larger droplets, which may compromise deposition uniformity (Privitera et al., 2023; Schick, 2008)

Another important parameter for evaluating spray characteristics is the Relative Span Factor (RSF), which indicates the uniformity of the droplet size distribution. The RSF is defined by the equation (1):

$$RSF = \frac{Dv0.9 - Dv0.1}{Dv0.5} \qquad \text{(Equation 1)}$$

A higher RSF value indicates greater variability in droplet size distribution, potentially leading to increased drift and uneven coverage. Conversely, a lower RSF value suggests more uniform droplet distribution, reducing drift and improving spray deposition (Privitera et al., 2023).

5. OBJECTIVES

The main goal of this thesis is to evaluate the effects of DJI Agras T40 drone operational parameters on spray characteristics in both a simulated experimental area and a peach orchard. The specific objective of this study is to:

1. Evaluate the effects of a DJI Agras T40 drone operational parameters, including application volume, flight height, droplet size, and operation mode on spray coverage, droplet density, droplet diameter, and droplet size uniformity in a simulated experimental area.
2. Determine the optimal DJI Agras T40 operational parameters, such as application volume, flight height, and droplet size for maximizing spray coverage across three operation modes (standard, fruit tree, and spinning) in a simulated experimental area.
3. Evaluate spray coverage variability at different positions within a simulated canopy structure, including center, southeast, southwest, south, northeast, northwest, and north, to determine spatial variability.

4. Assess the effects of optimized DJI Agras T40 operational parameters (application volume, flight height, and droplet size) across three operation modes (fruit tree, spinning, and standard) on spray coverage, droplet density, droplet diameter, and droplet size uniformity in a peach orchard.
5. Compare drone performance with that of a Jacto Arbus 2000 air-blast sprayer in a peach orchard.
6. Analyze spray coverage and droplet density across different canopy layers (upper, middle, and lower) and sampling locations (center, north, east, south, and west) within peach trees to determine spatial variability.

Chapter II

Optimization of drone operational parameters to enhance pest management efficiency in fruit tree orchards

Abstract

The use of unmanned aerial vehicles (UAVs), or drones, offers a promising alternative to conventional pesticide application methods, particularly in fruit tree orchards. This study evaluated the effects of key drone operational parameters (operation mode, application volume, flight height, and droplet size) on spray coverage, droplet density, droplet diameter, and droplet size uniformity using a DJI Agras T40 drone in a simulated orchard canopy. Three operation modes (standard, fruit tree, and spinning) were tested across two levels each of application volume (37.4 and 74.8 L/ha), flight height (3 and 5 m), and droplet size (150 and 300 μm). Results showed that the spinning mode achieved the highest mean of spray coverage (20.81%) and droplet density (172.44 drops/cm²), while the standard mode provided the most uniform spatial distribution. Optimal parameter configurations varied by mode: in standard mode, a 74.8 L/ha application volume, 3 m flight height, and 150 μm droplet size maximized coverage; in fruit tree mode, 74.8 L/ha, 5 m, and 300 μm were optimal; and in spinning mode, 74.8 L/ha, 3 m, and 300 μm achieved the best results. These findings highlight the importance of optimizing drone operational parameters to enhance spray performance, reduce chemical use, and thus minimize environmental impact. The results provide a foundation for developing adaptive drone-based spray systems and advancing precision agriculture in orchard management.

1. INTRODUCTION

Fruit and vegetable production represents a significant portion of agricultural output, accounting for almost 25% of the total agricultural production in the United States (USDA, 2024). In 2022, sales of fruits, tree nuts, and berries reached $34.2 billion, with almonds leading production, followed by grapes and pecans (USDA, 2022). Despite this, global fruit production faces substantial losses, with an estimated 78% attributed to pests and diseases (Luo et al., 2022; Sharma et al., 2019; Tudi et al., 2021).

Pesticides remain essential for protecting crops against insects, pests, diseases, and weeds, ensuring reliable yields (Sharma et al., 2019). However, overuse and improper application methods have raised concerns about human health and environmental pollution (Hüesker & Lepenies, 2022; Sookhtanlou et al., 2022; Tudi et al., 2021). Studies indicate that 74.6% of potato farmers in Iran and 70.6% of apple farmers in China exceed recommended pesticide dosages, contributing to unnecessary environmental contamination and increased production costs (Cai et al., 2021; Sookhtanlou et al., 2022).

Emerging technologies, including unmanned aerial vehicles (UAVs), commonly known as drones, offer sustainable and efficient alternatives to conventional pesticide application methods, such as air-blast sprayers (Gao et al., 2020; García-Munguía et al., 2024a; Mahmud et al., 2021). Drones offer several advantages, including reduced pesticide use, precise targeting, and minimized human exposure to hazardous chemicals. These benefits collectively reduce chemical waste, conserve water, save time, and decrease operational costs (Sahni et al., 2024; Wei, Li, et al., 2023; Wu et al., 2024).

Recent studies have demonstrated the comparable or superior efficacy of drones compared to conventional pesticide application methods, particularly in achieving better canopy penetration and coverage in hard-to-reach areas (Li et al., 2021; Arakawa & Kamio, 2023). For instance, (Arakawa & Kamio, 2023) found that pesticide application efficacy on chestnut trees was equivalent when applied using drones, air-blast sprayers, or high-pressure sprayers. Similarly, a study on almond trees compared drone spray deposition with conventional ground sprayers. While the ground method achieved higher overall coverage, drones delivered superior coverage at the top of the tree canopy, demonstrating their potential as complementary tool to ground sprayers (Li et al., 2021).

In drone spraying, droplet distribution on the target canopy is a critical metric for evaluating spraying performance. Improper droplet deposition can lead to pesticide waste, reduced effectiveness, environmental pollution, or even poisoning (Meng et al., 2020). Factors such as spray volume (G. Wang, Lan, Qi, et al., 2019), droplet size (S. Chen et al., 2020), flight height (S. Chen et al., 2017), and flight velocity significantly influence droplet distribution (Qin et al., 2018; Tang et al., 2018). Recently, advancements in drone technology have introduced spraying operation mode specifically designed for orchards, aiming to enhance deposition efficacy in fruit trees (Shan et al., 2024b). However, this operation mode has yet to be extensively explored (García-Munguía et al., 2024a). Therefore, the effects of drone operational parameters must be thoroughly characterized and properly optimized to obtain adequate and homogeneous spray deposition.

In this context, this study aimed to evaluate the effects of drone operational parameters (operation mode, application volume, flight height, and droplet size) on spray coverage, droplet density, droplet diameter, and droplet size uniformity. The study further identified optimal operational parameters for maximizing spray coverage across three operation modes (standard, fruit tree, and spinning). Spatial variability in spray distribution was also analyzed by assessing spray coverage at various positions within a simulated canopy structure, including the center, southeast, southwest, south, northeast, northwest, and north.

2. MATERIALS AND METHODS

2.1. Experimental equipment

A DJI Agras T40 drone sprayer (SZ DJI Technology Co., Shenzhen, China), an eight-motor coaxial multi-rotor drone, was used for all spraying experiments (Figure 1).

Figure 3. The DJI Agras T40 drone sprayer used in the spraying experiments.

The DJI Agras T40 features a 40 L tank capacity and an effective spray width of 11 m when flying at 7m/s at an altitude of 2.5 m. It utilizes a dual-atomized spray system, producing droplets ranging from 50 to 500 µm, with each nozzle capable of a maximum flow rate of 6 L/min (DJI, 2022). Table 2 summarizes the specifications of the DJI Agras T40.

Table 2. Specifications of the DJI Agras T40.

Parameter	Specification
Type	Eight-motor coaxial multi-rotor
Dimensions (L x W x H)	2800 mm × 3150 mm × 780 mm
Total weight (without battery)	38 kg
Total weight (with battery)	50 kg

Battery capacity	30,000 mAh
Tank capacity	40 L
Max speed	10 m/s
Droplet size range	50-500 µm
Spraying system	Dual Atomized Spraying System
Max effective spray width	11 m (at 2.5 m altitude, 7m/s flight speed)
Max flow rate	6 L/min per nozzle
Hovering time (without payload)	18 min
Hovering and spraying (with full payload)	7 min
Max flight radius	2000 m
Max wind resistance	6 m/s

For precision positioning, the DJI T40 was operated with a GNSS mobile base station (Model D-RTK 2), achieving horizontal and vertical accuracies within ±10 cm. The drone was equipped with an omnidirectional radar and a terrain-following system capable of managing inclines up to 30°. Flight control and spray management were conducted using the DJI Agras intelligent remote controller, integrated with flight planning software. Orthomosaics of the test area were generated using DJI Terra software (SZ DJI Technology Co., Shenzhen, China) to facilitate flight planning.

2.2. Experimental conditions

The experiments were conducted at the Auburn University Turfgrass Unit in Auburn, AL (32°34'41.58"N, 85°30'3.73"W) on July 12 and 30, 2024. The test site, measuring 120 m in length and 20 m in width, featured a synthetic grass surface. Meteorological data, including wind speed (m/s), temperature (°C), and relative humidity (%), were recorded every 10 s using a Kestrel 5500 weather meter (Kestrel Instruments, Boothwyn, PA, USA), installed on a tripod at a height of 1.8 m. Weather conditions were averaged across treatments on each application day (Table 3).

Table 3. Meteorological conditions during the application days

Parameter	12-July	30-July
Temperature (°C)	28.55 ± 1.27[a]	28.10 ±1.16

Relative humidity (%)	71.32 ± 10.68	84.70 ± 4.14
Wind speed (m/s)	1.10 ± 0.62	0.95 ± 0.19

[a] Results are presented as mean ± standard error.

All experiments were performed under acceptable wind conditions, with wind speeds below 2 m/s and wind angles up to ± 15°, in accordance with the ASAE S386.2 standard (American Society of Agricultural Engineers, 1988).

2.3. Experimental design

A four-factorial experimental design was conducted to evaluate the effects of flight height (3 and 5 m above ground level), droplet size (150 and 300 μm), application volume (37.4 and 74.8 L/ha), and operation mode (standard, fruit tree, and spinning) on spray coverage, droplet density, droplet diameter, and droplet size uniformity. A total of 24 treatments were tested, with each treatment replicated four times, resulting in 96 flights. Parameters were selected based on manufacturer recommendations (DJI, 2022) and ASABE S572.1 standards (American Society of Agricultural Engineers, 1988).

2.4. Experimental layout

Four circular plastic structures, each 6 m in diameter, were constructed on the ground to simulate fruit tree canopy areas. Each structure consisted of three intersecting plastic tubes, serving as a framework for attaching Kromekote white paper (KWP) (The Paper Mill Store, Neenah, WI, USA) cards, which were strategically positioned at seven locations: center, southeast, southwest, south, northeast, northwest, and north. The KWP cards were selected to simulate the surface characteristics of fruit tree leaves.

KWP cards were spaced at 1 m intervals, resulting in a total of 19 cards per structure (Figure 4a). The structures, spaced 10 m apart, represented independent replications (Figure 4b).

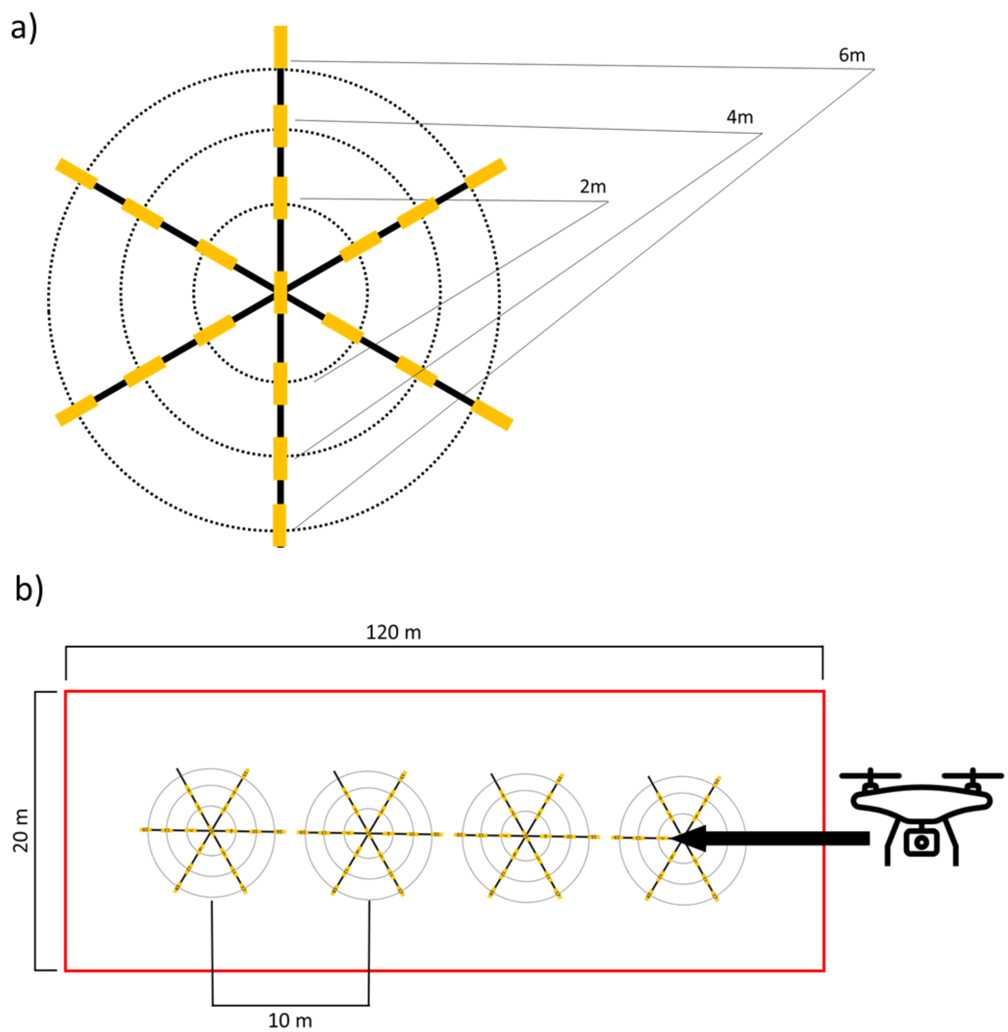

Figure 4. a) Schematic circular plastic structure used to simulate fruit tree canopy areas. Kromekote white paper (KWP) cards (yellow) were evenly distributed to capture spray deposition. b) Experimental layout illustrating four structures spaced 10 m apart. The arrow indicates the drone's flight path during application.

2.5. Data collection and processing

A water-based solution containing Vision Pink™ dye (GarrCo Products, Converse, IN, USA) at a concentration of 20 mL/L was used for all experiments. The solution was sprayed from the drone as it flew over the center of each simulated canopy structure (Figure 4b), using three different operation modes: standard, fruit tree, and spinning.

In the standard mode, the drone follows a continuous flight path, applying the spray solution at a predefined volume rate along its trajectory. In the fruit tree mode, the drone hovers upon reaching the center of a target area, activates its nozzles, and sprays the solution at the designated volume rate. Once spraying is complete, the drone continues along the route to the next target area and repeats the process. This operation is repeated until all target areas within the operational zone are sprayed. In the spinning mode, the drone hovers at the center of a target area, activates its nozzles, and rotates around its central axis while spraying the solution at the specified volume rate. After completing the spraying at one target area, the drone moves to the next target area and repeats the procedure. This cycle continues until all target areas within the operational zone are sprayed.

After each experiment, KWP cards were collected, stored in pre-labeled adhesive note blocks, and sealed in plastic bags with silica pouches to prevent moisture contamination.

The KWP cards were scanned using an Epson Perfection V39II flatbed scanner (Epson America Inc., Long Beach, CA, USA) at a resolution of 1200 dpi. The scanned images were analyzed using the AccuStain software (Version 0.32, developed by Matt Gill, University of Illinois at Urbana-Champaign, USA). The software automatically processed the scanned images using its default configuration for cast-coat papers and analyzed key spray deposition parameters, including spray coverage, droplet density, droplet diameter, and droplet size uniformity.

Spray coverage (%) was calculated as the ratio of the spray deposits area (the area covered by stains) to the total area analyzed on the KWP cards (Gill, 2024). Droplet density (drops/cm^2) was determined by calculating the number of droplets deposited per unit area on the KWP cards (Gill, 2024). The droplet diameter (μm) corresponding to 10% ($D_{v0.1}$), 50% ($D_{v0.5}$, also known as Volume Median Diameter or VMD), and 90% ($D_{v0.9}$) of the spray volume were also determined. The Dv0.1 indicates that 10% of the spray volume comprises droplets smaller than Dv0.1. For instance, if Dv0.1 is 200 µm, 10% of the spray volume consists of droplets that are 200 µm or smaller. Dv0.9 represents the droplet diameter where 90% of the spray volume consists of droplets smaller than Dv0.9. Dv0.5 is the midpoint of the droplet size distribution, where half of the spray volume consists of droplets smaller than Dv0.5, and the other half consists of larger droplets (Gill, 2024).

The droplet size uniformity was determined by the relative span factor (RSF), calculated using equation (1) (Gill, 2024).

$$RSF = \frac{Dv0.9 - Dv0.1}{Dv0.5} \qquad \text{Equation (1)}$$

2.6. Statistical analysis

Data was analyzed using a generalized linear mixed model with the PROC GLIMMIX procedure in SAS (version 9.04.01M7P08062020). Flight height, droplet size, application volume, operation mode, and their interactions were used as fixed effects for the analysis of spray coverage, droplet density, droplet diameter (Dv0.1, Dv0.5, Dv0.9), and droplet uniformity (RSF). Data was checked for normality and homogeneity of variance. Analysis of variance was conducted to evaluate the significance of the fixed effects and their interactions. When the F-value of the analysis of variance was significant, least-square mean comparisons were performed to identify differences between treatments, using Tukey's test with a *p*-value of 0.05.

Additionally, a heatmap was created using SAS to visually represent the effects of drone operational parameters on spray coverage for each operation mode (standard, fruit tree, and spinning). The highest spray coverage values achieved for each mode were identified, and an orthogonal contrast analysis was conducted to statistically compare these maximum coverage values among the three operation modes.

3. RESULTS

3.1. Spray coverage

The main effects of operation mode, application volume, and flight height significantly influenced spray coverage ($p \leq 0.01$), whereas droplet size did not have a significant effect ($p > 0.05$). Among the operation modes (Figure 5a), the spinning mode resulted in the highest average spray coverage (20.81%), followed by the fruit tree (18.26%) and the standard (17.04%) modes. Higher application volumes (74.8 L/ha) resulted in greater spray coverage than lower application volumes (37.4 L/ha) (Figure 5b). A lower flight height of 3 m resulted in greater spray coverage compared to 5 m (Figure 5c). Although a slight increase in spray coverage was observed with smaller droplet sizes (150 μm) (Figure 5d), the effect of droplet size on spray coverage was not significant ($p > 0.05$). However, significant interactions with operation mode and application volume ($p \leq 0.05$) suggest that droplet size influences spray coverage under specific conditions.

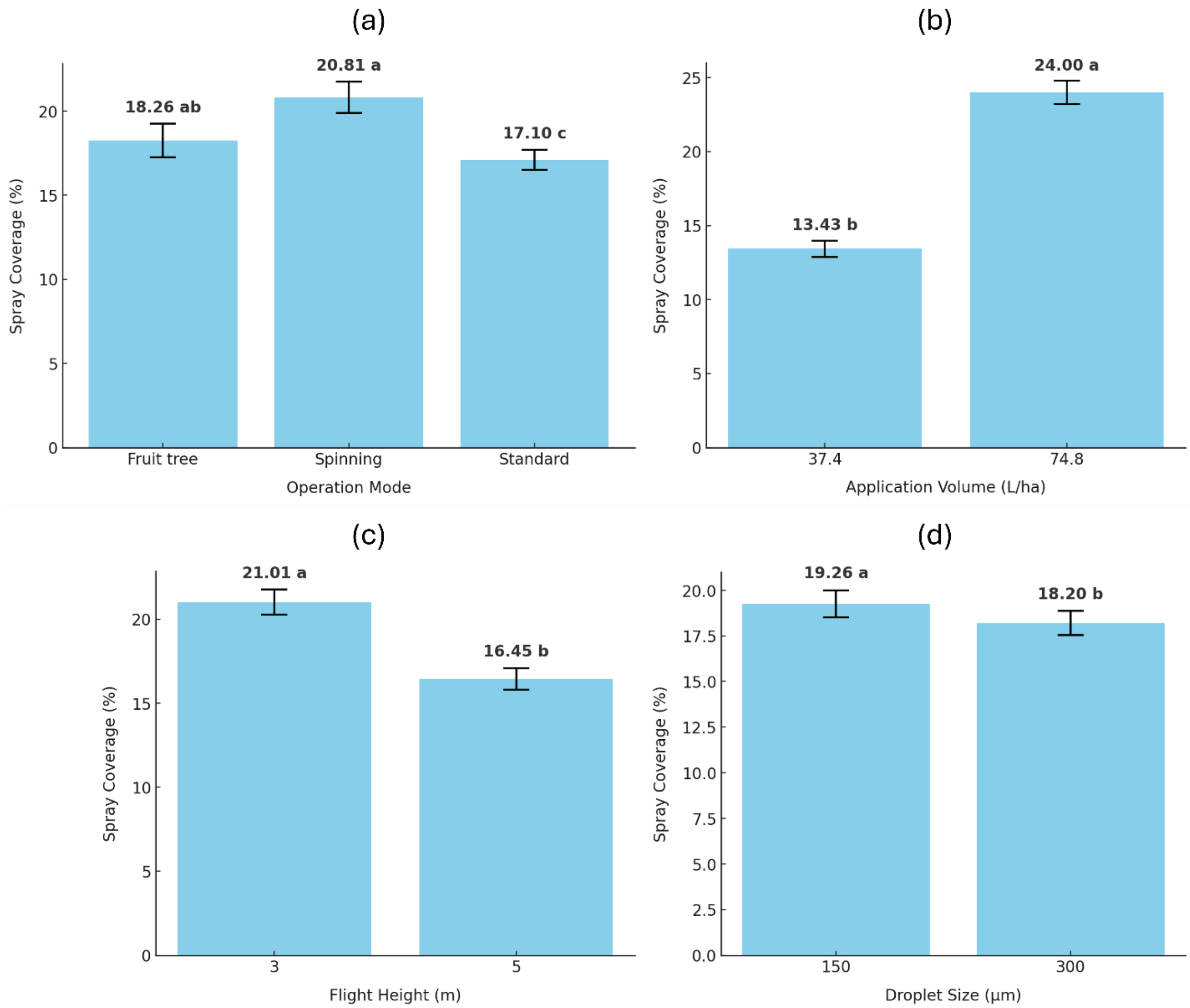

Figure 5. Main effects of (a) operation mode, (b) application volume, (c) flight height, and (d) droplet size on spray coverage. Bar graphs represent the average spray coverage for each factor, with whiskers indicating the error range. Means with the same lowercase letters are not significantly different as determined by Tukey's test ($\alpha = 0.05$).

Spray coverage was also significantly influenced by the two-way interactions of operation mode and application volume ($p \leq 0.01$), operation mode and droplet size ($p \leq 0.05$), and application volume and droplet size ($p \leq 0.01$). As shown in Figure 6(a), increasing the application volume from 37.4 L/ha to 74.8 L/ha significantly enhanced spray coverage across all operation modes. For example, in the standard mode, coverage increased from 9.05% to 24.0%, while in the fruit tree and spinning modes, it increased from 15.0% to 21.5% and from 16.2% to 25.4%, respectively.

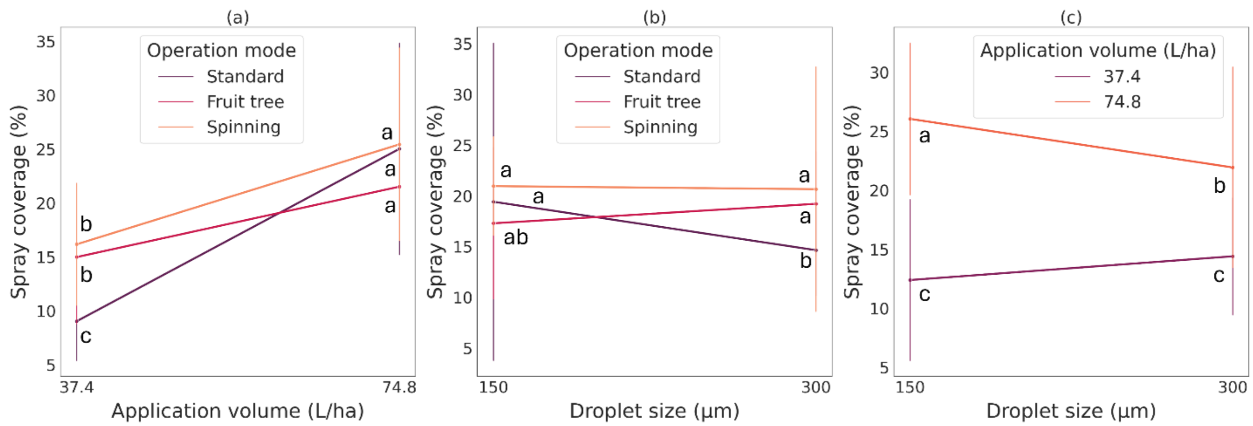

Figure 6. Interaction effects of (a) operation mode and application volume, (b) operation mode and droplet size, and (c) application volume and droplet size on spray coverage. Vertical bars indicate standard errors. Means with the same lowercase letters are not significantly different, as determined by Tukey's test ($\alpha = 0.05$).

Figure 6(b) illustrates the interaction between operation mode and droplet size on spray coverage. In the spinning mode, increasing droplet size from 150 µm to 300 µm slightly decreased coverage from 21.0% to 20.7%. A similar trend was observed in the standard mode (from 19.4% to 14.7%), whereas in the fruit tree mode, coverage increased from 17.3% to 19.2%.

The interaction between application volume and droplet size is shown in Figure 6(c). At a lower application volume (37.4 L/ha), spray coverage was 12.4% for 150 µm droplets and 14.4% for 300 µm droplets. In contrast, at a higher application volume (74.8 L/ha), coverage decreased from 26.0% with 150 µm droplets to 21.9% with 300 µm droplets.

Additionally, three-way interactions significantly influenced spray coverage, including operation mode, droplet size, and application volume ($p \leq 0.01$); operation mode, droplet size, and flight height ($p \leq 0.01$); operation mode, application volume, and flight height ($p \leq 0.01$); and droplet size, application volume, and flight height ($p \leq 0.05$). Table 4 presents these effects. Spray coverage was higher at an application volume of 74.8 L/ha compared to 37.4 L/ha across all operation modes and droplet sizes. Specifically, with 150 µm droplets, the standard mode resulted in the highest spray coverage at 74.8 L/ha (32.4%), followed by the fruit tree (23.1%), and spinning (22.7%) modes. At 37.4 L/ha, the spinning mode had the highest coverage (19.3%), with the fruit tree and standard modes at 11.6% and 6.4%, respectively. When applying 300 µm droplets, the fruit tree mode exhibited similar coverage values at 37.4 L/ha (18.5%) and 74.8 L/ha (20.0%), while the spinning mode increased from 13.1% to 28.3% and the standard mode from 11.7 to 17.6%.

Table 4. Effects of operation mode, droplet size, application volume, and flight height on spray coverage.

Spray coverage (%)				
Fruit tree				
Droplet size (µm)	**Application volume (L/ha)**		**Flight height (m)**	
	37.4	**74.8**	**3**	**5**
150	11.51^{bB}	23.10^{aA}	19.68^{aA}	14.91^{bB}
300	18.48^{aA}	19.96^{aA}	19.05^{aA}	19.39^{aA}
Spinning				
Droplet size (µm)	**Application volume (L/ha)**		**Flight height (m)**	
	37.4	**74.8**	**3**	**5**
150	19.26^{aA}	22.67^{bA}	20.65^{bA}	21.28^{aA}
300	13.10^{bB}	28.22^{aA}	27.16^{aA}	14.16^{bB}
Standard				
Droplet size (µm)	**Application volume (L/ha)**		**Flight height (m)**	
	37.4	**74.8**	**3**	**5**
150	6.43^{bB}	32.41^{aA}	22.4^{aA}	16.66^{aB}
300	11.70^{aB}	17.64^{bA}	17.12^{bA}	12.23^{bB}

Similar lowercase letters in the same column indicate no significant differences between droplet sizes within each operation mode as determined by Tukey's test ($p > 0.05$). Similar uppercase letters in the same line indicate no significant differences between application volumes or flight heights within each operation mode as determined by Tukey's test ($p > 0.05$).

Spray coverage varied with different operation modes, droplet sizes, and flight height (Table 4). In the fruit tree mode, coverage decreases as flight height increases, with values ranging from 19.68% at 3 m and 14.91% at 5 m for 150 µm droplets, while for 300 µm droplets, coverage remained relatively stable (19.05% at 3 m and 19.39% at 5 m). In the spinning mode, 150 µm droplets resulted in coverage of 20.65% at 3 m and 21.28% at 5 m, while 300 µm droplets exhibited a significant decrease from 27.16% at 3 m to 14.16% at 5 m. In the standard mode, coverage decreased with higher flight heights, with 150 µm droplets showing a decrease from 22.40% at 3 m to 16.66% at 5 m, and 300 µm droplets following a similar trend, decreasing from 17.12% to 12.23%.

Although the four-way interaction among operation mode, application volume, droplet size, and flight height were not significant ($p > 0.05$), optimal conditions for maximizing spray coverage were identified (Figure 7). For the spinning mode, spray coverage ranged from 9.68% to 37.80%, with optimal coverage achieved at a 74.8 L/ha application volume, 3 m flight height, and 300 µm droplets (Figure 7). In the fruit tree mode, coverage ranged from 7.63% to 24.52%, with optimal conditions at an application volume of 74.8 L/ha, a flight height of 5 m, and a droplet size of 300 µm, achieving 24.52% coverage (Figure 7). In the standard mode, coverage varied between 6.29% and 37.80%, with the optimal configuration for maximizing spray coverage at a 74.8 L/ha application volume, 3 m flight height, and 150 µm droplet size, resulting in 37.80% coverage. These results highlight the importance of selecting appropriate flight heights and droplet sizes to maximize spray coverage in each operation mode.

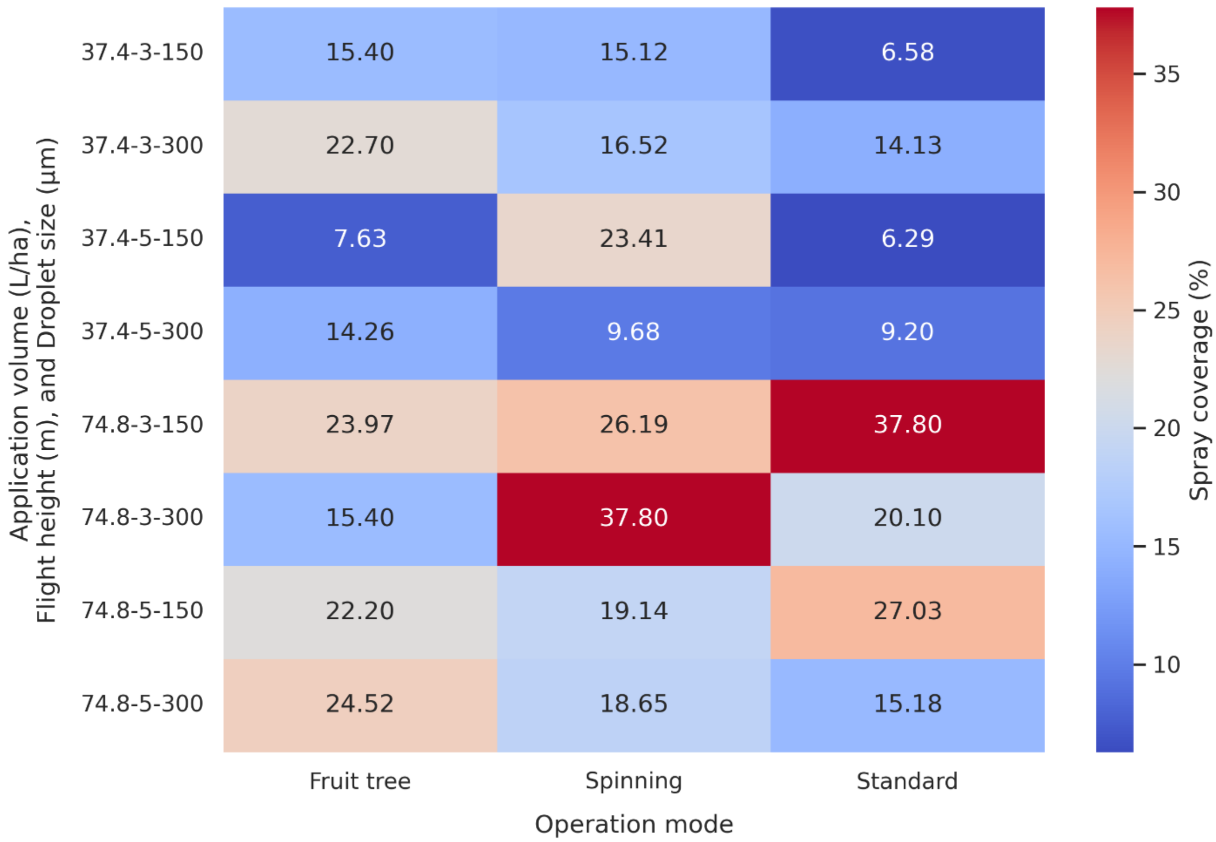

Figure 7. Heatmap illustrating the interaction between operation mode, droplet size, flight height, and application volume on spray coverage. Each cell displays the average spray coverage value for that treatment combination, with color intensity corresponding to the magnitude of spray coverage. Warmer colors indicate higher spray coverage, while cooler colors indicate lower coverage.

A contrast analysis comparing the optimal treatments for each operation mode on spray coverage (Table 5) revealed no significant difference between the standard mode and spinning mode ($p > 0.05$), indicating that both modes are equally effective in maximizing spray coverage. However, the fruit tree mode exhibited significantly lower coverage than both the spinning and standard modes ($p \leq 0.01$).

Table 5. Contrast between treatments with the highest spray coverage for each operation mode.

Operation mode comparison	Sum of square	F value	*p*-value
Standard *vs* Spinning	0.000506	0	ns
Standard *vs* Fruit tree	6701.16	17.51	**
Spinning *vs* Fruit tree	6697.47	17.50	**

Level of significance (p-value): **, significant at $p \leq 0.01$; ns, nonsignificant.

3.2. Droplet density

Statistical analysis showed that all main effects were significant ($p \leq 0.01$) for droplet density, with additional two-way and three-way interactions ($p \leq 0.05$) indicating complex relationships among these factors. Among operation modes, the spinning mode resulted in the highest droplet density (172.44 drops/cm^2), followed by the fruit tree mode (140.47 drops/cm^2), with the standard mode showing the lowest density (77.83 drops/cm^2) (Figure 8a). Increasing the application volume from 37.4 L/ha to 74.8 L/ha significantly enhanced droplet density from 114.00 drops/cm^2 to 146.35 drops/cm^2 (Figure 8b). Similarly, a lower flight height (3 m) led to higher droplet density (136.53 drops/cm^2) compared to 5 m (123.82 drops/cm^2) (Figure 8c). Smaller droplet sizes (150 μm) resulted in higher densities (141.28 drops/cm^2) than larger droplets (300 μm) (119.07 drops/cm^2) (Figure 8d).

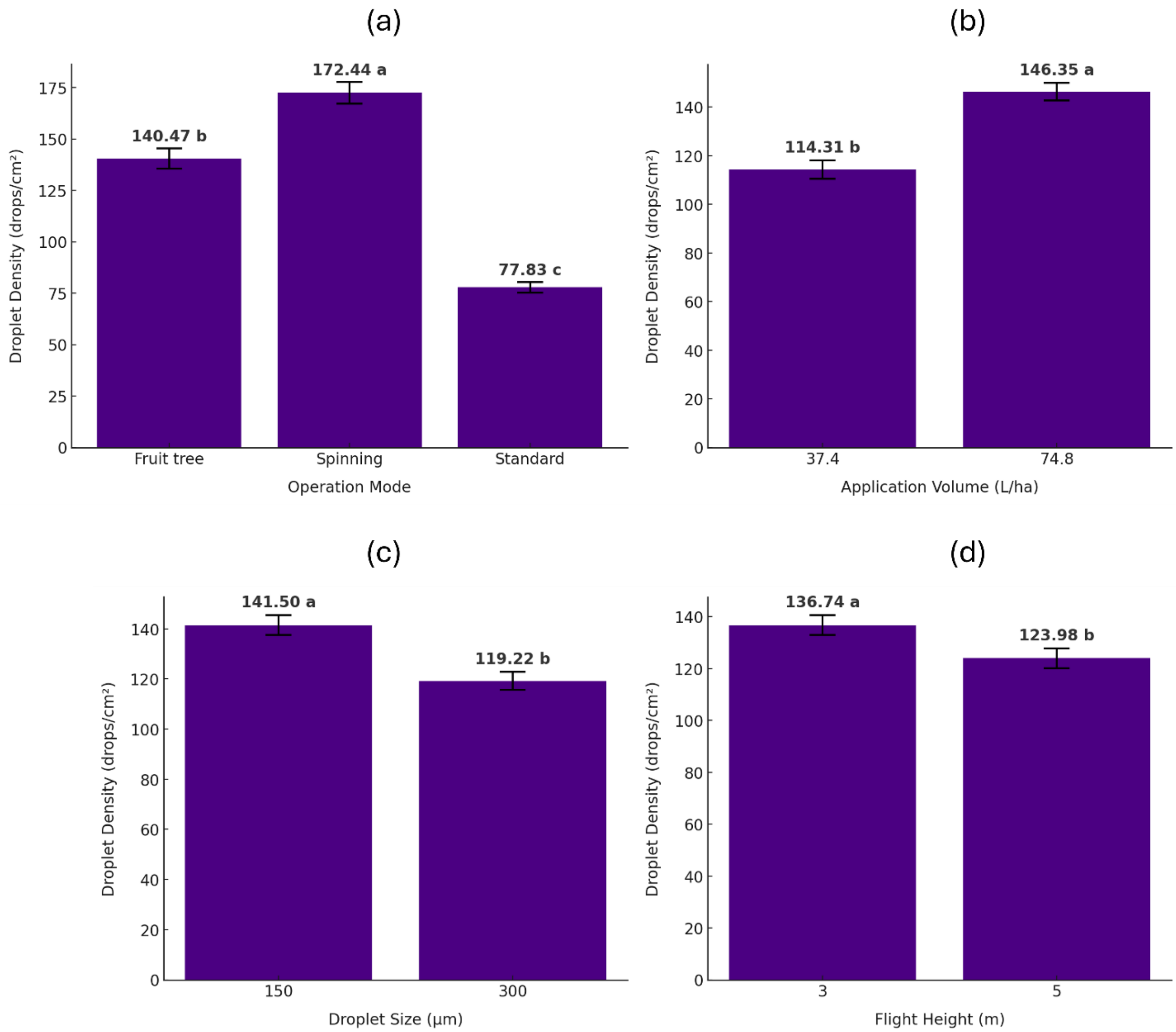

Figure 8. Main effects of (a) operation mode, (b) application volume, (c) droplet size, and (d) flight height on droplet density. Bar graphs represent the average droplet density for each factor, with the whiskers indicating the standard error. Similar lowercase letters indicate no significant differences among treatment levels ($p > 0.05$), as determined by Tukey's test.

The interaction effects of operation mode and application volume, droplet size and application volume, and droplet size and flight height on droplet density were statistically significant ($p \leq 0.05$), highlighting the complex relationships among these factors. Figure 9(a) illustrates that at a lower application volume (37.4 L/ha), the spinning mode produced the highest droplet density (160.78 drops/cm²), followed by the fruit tree mode (130.01 drops/cm²) and standard mode (51.23 drops/cm²). At a higher application volume (74.8 L/ha), droplet density increased across all operation modes, reaching 184.11 drops/cm² in spinning mode, 150.93 drops/cm² in fruit tree mode, and 104.01 drops/cm² in standard mode.

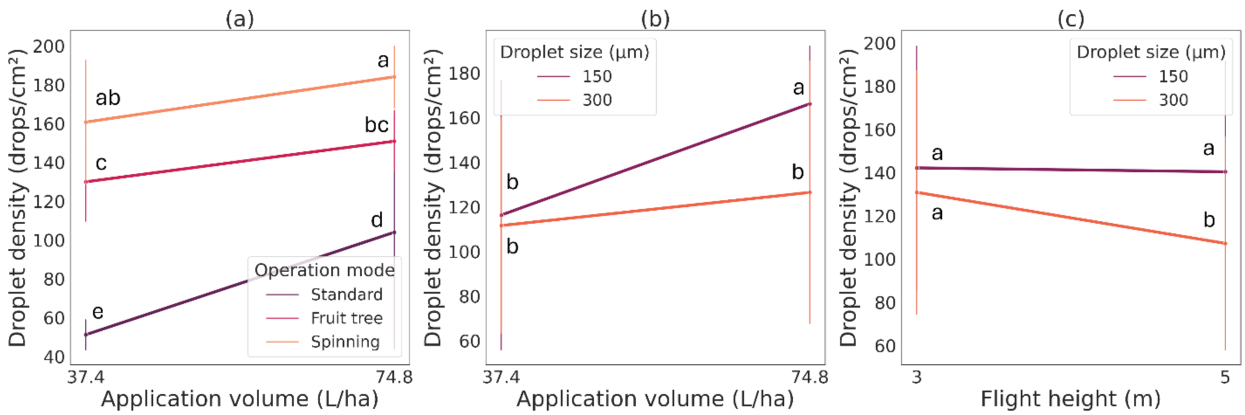

Figure 9. Interaction effects of (a) operation mode and application volume, (b) droplet size and application volume, and (c) droplet size and flight height on droplet density. Error bars indicate the standard deviation. Similar lowercase letters indicate no significant differences ($p > 0.05$) among treatments within each panel, as determined by Tukey's test.

For smaller droplets (150 µm), increasing the application volume from 37.4 L/ha to 74.8 L/ha significantly increased droplet density from 116.36 drops/cm² to 166.22 drops/cm² (Figure 9b). In contrast, for larger droplets (300 µm), the increase was less pronounced (from 111.65 to 126.49 drops/cm²). In addition, droplet density decreased as flight height increased (Figure 9c). At 3 m, smaller droplets (150 µm) resulted in a droplet density of 142.19 drops/cm², while larger droplets (300 µm) reduced it to 130.88 drops/cm². At 5 m, overall density was lower, with smaller droplets yielding 140.38 drops/cm² and larger droplets reducing to 107.26 drops/cm².

Droplet density was also significantly influenced by the three-way interactions of operation mode, droplet size, and application volume ($p \leq 0.01$), and operation mode, application volume, and flight height ($p \leq 0.05$). For the fruit tree mode, droplet density increased with higher application volume (Table 5). At 37.4 L/ha, larger droplets (300 µm) produced higher droplet density (143.65 drops/cm²) than smaller droplets (150 µm, 116.37 drops/cm²). At 74.8 L/ha, droplet density remained stable between droplet sizes (151.30 drops/cm² for 150 µm droplets and

150.57 drops/cm² for 300 µm droplets). Flight height influenced droplet density (Table 6), with 3 m yielding higher values (141.03–147.72 drops/cm²) than 5 m (118.99–154.14 drops/cm²). In the spinning mode, smaller droplets (150 µm) resulted in higher droplet density (Table 6). At 37.4 L/ha, droplet density reached 183.08 drops/cm² for 150 µm but decreased to 138.48 drops/cm² for 300 µm droplets. Increasing the application volume to 74.8 L/ha led to the highest droplet density observed (193.05 drops/cm² for 150 µm and 175.17 drops/cm² for 300 µm). Lower flight heights (3 m) produced greater droplet density (170.34–193.90 drops/cm²) compared to 5 m (151.22–174.32 drops/cm²). The standard mode exhibited the lowest overall droplet density, particularly at 37.4 L/ha, where values remained below 53 drops/cm² for both droplet sizes. At 74.8 L/ha, droplet density increased for 150 µm droplets (154.29 drops/cm²), while the increase was minimal for 300 µm droplets (53.73 drops/cm²). Flight height also had a significant effect, with higher droplet density observed at 3 m (48.94 - 117.28 drops/cm²) compared to 5 m (53.51 - 90.74 drops/cm²).

Table 6. Effects of operation mode, droplet size, application volume, and flight height on droplet density.

Droplet density (drops/cm2)				
Fruit tree				
Application volume (L/ha)	**Droplet size (µm)**		**Flight height (m)**	
	150	**300**	**3**	**5**
37.4	116.37^{bB}	143.65^{aA}	141.03^{aA}	118.99^{bA}
74.8	151.3^{aA}	150.57^{aA}	147.72^{aA}	154.14^{aA}
Spinning				
Application volume (L/ha)	**Droplet size (µm)**		**Flight height (m)**	
	150	**300**	**3**	**5**
37.4	183.08^{aA}	138.48^{bB}	170.34^{bA}	151.22^{aA}
74.8	193.05^{aA}	175.17^{aA}	193.9^{aA}	174.32^{aA}
Standard				
Application volume (L/ha)	**Droplet size (µm)**		**Flight height (m)**	
	150	**300**	**3**	**5**
37.4	49.62^{bA}	52.83^{aA}	48.94^{bA}	53.51^{bA}
74.8	154.29^{aA}	53.73^{aB}	117.28^{aA}	90.74^{aB}

Similar lowercase letters in the same column indicate no significant differences between volumes within each operation mode as determined by Tukey's test ($p > 0.05$). Similar uppercase letters in the same line indicate no significant differences between droplet size or flight heights within each operation mode as determined by Tukey's test ($p > 0.05$).

Although the four-way interaction among operation mode, application volume, droplet size, and flight height were not statistically significant ($p > 0.05$), notable trends emerged in droplet density patterns. The standard mode exhibited the lowest droplet density, ranging from 41.26 to 171.46 drops/cm². At an application volume of 37.4 L/ha, the highest droplet density (57.98 drops/cm²) occurred at a 5 m flight height with 150 µm droplets, whereas increasing the application volume to 74.8 L/ha led to a maximum droplet density of 171.46 drops/cm² at 3 m and 150 µm droplets. In the fruit tree mode, droplet density ranged from 105.51 to 167.82 drops/cm². At a 37.4 L/ha, the highest droplet density (154.82 drops/cm²) was observed at a 3 m flight height with 300 µm droplets. However, at 74.8 L/ha, the highest density (167.82 drops/cm²) was achieved at a 5 m flight height with 150 µm droplets. The spinning mode produced the highest droplet density, ranging from 115.79 to 198.91 drops/cm². At 37.4 L/ha, the highest density (186.64 drops/cm²) occurred at 5 m with 150 µm droplets. When the application volume was increased to 74.8 L/ha, the highest recorded density (198.91 drops/cm²) was achieved at a 3 m with 150 µm droplets.

3.3. Droplet diameter (Dv0.1, Dv0.5, and Dv0.9)

The droplet diameter was significantly influenced by operation mode, application volume, flight height, and droplet size ($p \leq 0.01$), with multiple interaction effects observed among these factors. Among the operation modes (Figure 10a), the standard mode exhibited the largest droplet diameters across all percentiles (Dv0.1: 196.65 µm, Dv0.5: 346.91 µm, and Dv0.9: 513.43 µm). In contrast, the fruit tree and spinning modes produced smaller droplets, with no statistically significant differences between them for the Dv0.1 percentile. For the Dv0.5 and Dv0.9

percentiles, the spinning mode produced slightly, but still statistically significant bigger droplets (238.32 µm and 347.99 µm respectively) compared to the fruit tree mode.

The droplet size (150 µm and 300 µm) significantly influenced droplet distribution (Figure 10b). The larger droplet size (300 µm) produced greater droplet diameters across all percentiles (Dv0.1: 165.49 µm, Dv0.5 284.72 µm, and Dv0.9: 417.62 µm) compared to the 150 µm droplets (Dv0.1: 148.90 µm, Dv0.5 258.94 µm, and Dv0.9: 379.31 µm). Similarly, an increase in application volume from 37.4 L/ha to 74.8 L/ha resulted in larger droplet diameters across all percentiles (Figure 10c), suggesting that higher liquid volumes promote the formation of larger droplets. Increasing flight height from 3 m to 5 m led to a reduction in droplet diameter across all percentiles (Figure 10d). Specifically, Dv0.1 decreased from 162.20 to 152.10 µm, Dv0.5 from 180.48 to 263.18 µm, and Dv0.9 from 408.93 to 388.00 µm.

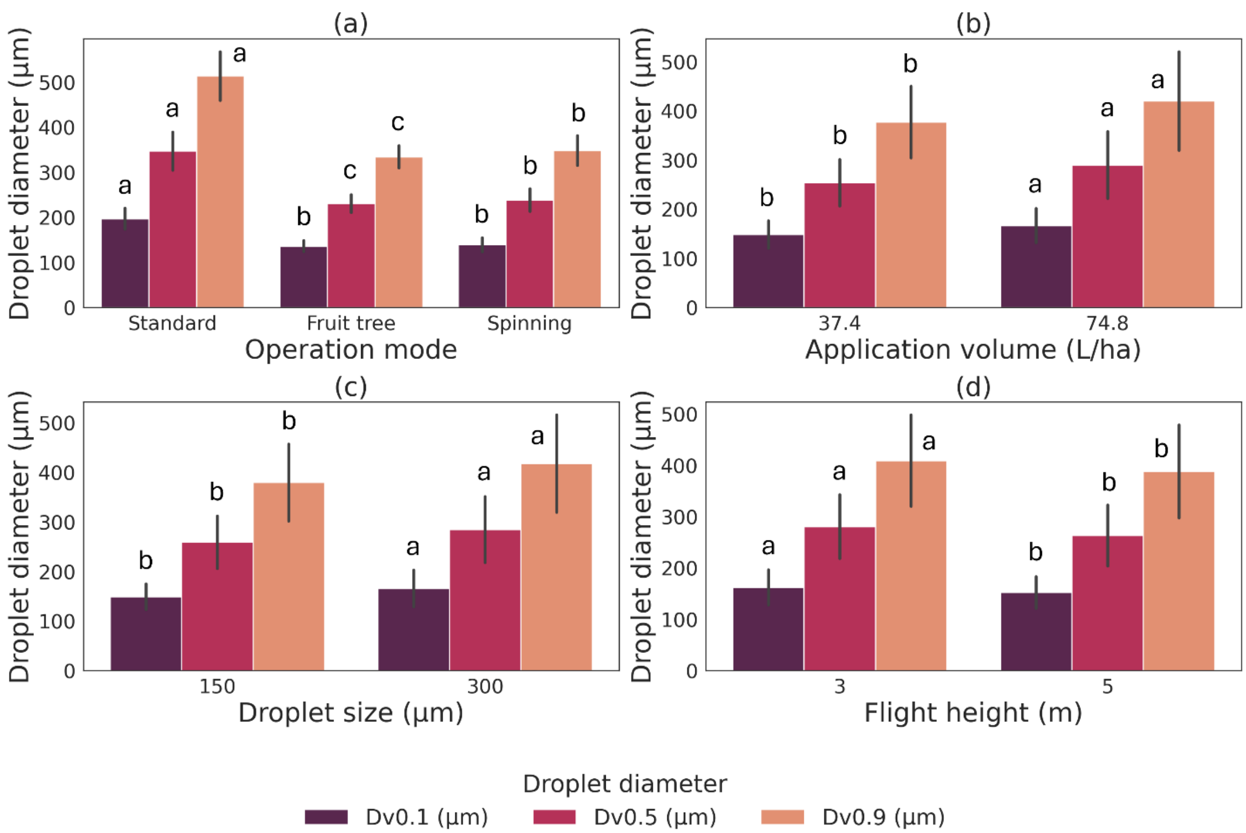

Figure 10. Main effects of (a) operation mode, (b) application volume, (c) droplet size, and (d) flight height on droplet diameter (Dv0.1, Dv0.5, and Dv0.9). Each bar represents the mean value, and error bars indicate the standard deviation. The legend denotes the droplet diameter percentiles: Dv0.1 (10% of volume is composed of droplets smaller than this size), Dv0.5 (median volume diameter), and Dv0.9 (90% of volume is below this size). Similar lowercase letters indicate no significant differences among treatment levels ($p > 0.05$), as determined by Tukey's test.

Additionally, three-way interactions significantly influenced droplet diameter, including operation mode, droplet size, and application volume ($p \leq 0.01$); operation mode, droplet size, and flight height ($p \leq 0.01$); and operation mode, application volume, and flight height ($p \leq 0.01$). Table 7 presents the interaction effects of operation mode, application volume, and flight height on droplet diameter.

Table 7. Effects of operation mode, application volume, and flight height on droplet diameter.

Operation mode	Application volume (L/ha)	Flight height (m)	Dv0.1 (µm)	Dv0.5 (µm)	Dv0.9 (µm)
Fruit tree	37.4	3	138.05^{ef}	235.55^{e}	342.02^{e}
		5	121.42^{g}	204.11^{f}	299.65^{f}
	74.8	3	140.72^{ef}	239.43^{e}	345.98^{e}
		5	143.69^{de}	241.96^{e}	348.26^{e}
Spinning	37.4	3	127.65^{fg}	223.29^{ef}	333.98^{e}
		5	136.83^{ef}	234.14^{e}	342.20^{e}
	74.8	3	157.53^{cd}	268.36^{d}	386.16^{d}
		5	133.88^{efg}	227.50^{e}	329.61^{e}
Standard	37.4	3	195.71^{b}	330.37^{b}	487.90^{b}
		5	168.94^{c}	296.22^{c}	456.43^{c}
	74.8	3	213.53^{a}	385.91^{a}	557.56^{a}
		5	208.43^{ba}	375.16^{a}	551.83^{a}

Similar lowercase letters indicate no significant differences between application volumes or flight heights within each operation mode and droplet size combination as determined by Tukey's test ($p > 0.05$).

At an application volume of 74.8 L/ha and a flight height of 3 m, the standard mode produced the largest droplet diameter (Dv0.1: 213.53 µm, Dv0.5: 385.91 µm, Dv0.9: 557.56 µm). In spinning mode, the highest values were recorded at a flight height of 3 m and 74.8 L/ha application volume (Dv0.1: 157.53 µm, Dv0.5: 268.36 µm, and Dv0.9: 386.16 µm. For the fruit tree mode, the highest droplet diameters were observed at a flight height of 5 m and an application volume of 74.8 L/ha (Dv0.1: 143.69 µm, Dv0.5: 241.96 µm, and Dv0.9: 348.26 µm.

Increasing the application volume from 37.4 L/ha to 74.8 L/ha resulted in an increase in droplet diameter across all operation modes. For instance, in standard mode at 3 m flight height, Dv0.1 increased from 195.71 µm to 213.53 µm, Dv0.5 from 330.37 µm to 385.91 µm, and Dv0.9 from 487.90 µm to 557.56 µm. Similar trends were observed for fruit tree and spinning modes, though with smaller droplet diameters. In contrast, increasing flight height from 3 m to 5 m generally led to a reduction in droplet diameter across all operation modes. For example, in standard mode at 74.8 L/ha, Dv0.1 decreased from 213.53 µm to 208.43 µm, Dv0.5 from 385.91 µm to 375.16 µm, and Dv0.9 from 557.56 µm to 551.83 µm. Similar trends were observed in fruit tree mode at 37.4 L/ha, where Dv0.1 decreased from 138.05 µm to 121.42 µm, Dv0.5 from 235.55 µm to 204.11 µm, and Dv0.9 from 342.02 µm to 299.65 µm.

3.4. Relative span factor (RSF)

The RSF, an indicator of droplet size uniformity, was significantly influenced by operation mode and application volume ($p \leq 0.01$), with additional two-way, three-way, and four-way interactions ($p \leq 0.05$). These interactions highlight the influence of combined parameters on droplet size uniformity, suggesting that RSF variability dependents not only on individual factors but also on their interactions.

The standard mode exhibited the highest RSF values under different conditions, indicating a less uniform droplet distribution, particularly at a flight height of 5 m with a droplet size of 150 µm and an application volume of 37.4 L/ha (RSF: 1.01). In contrast, the fruit tree and spinning modes showed lower RSF values, with minimal variation between droplet sizes and flight heights (Table 8).

Table 8. Effects of operation mode, application volume, droplet size, and flight height on relative span factor (RSF).

Operation mode	Application volume (L/ha)	Flight height (m)	Droplet size (µm)	RSF
Standard	37.4	3	150	0.90 bcd
			300	0.88 bcd
		5	150	1.01 a
			300	0.95 ab
	74.8	3	150	0.89 bcd
			300	0.91 bcd
		5	150	0.94 abcd
			300	0.91 bcd
Fruit tree	37.4	3	150	0.92 abcd
			300	0.87 bcd
		5	150	0.87 bcd
			300	0.90 bcd
	74.8	3	150	0.86 cd
			300	0.94 abcd
		5	150	0.91 bcd
			300	0.86 d
Spinning	37.4	3	150	0.93 abcd
			300	0.94 abc
		5	150	0.88 bcd
			300	0.90 bcd
	74.8	3	150	0.90 bcd
			300	0.86 cd
		5	150	0.86 cd
			300	0.88 bcd

Values with similar lowercase letters in the same column within operation mode indicate no significant differences ($p > 0.05$) by Tukey's test.

For the fruit tree mode, RSF values ranged between 0.86 and 0.94, indicating a more uniform droplet size distribution compared to the standard mode, particularly at an application volume of 74.8 L/ha with a droplet size of 300 µm and a flight height of 5 m. Similarly, in spinning mode, RSF values varied between 0.86 and 0.94, reflecting a more uniform droplet size distribution compared to the standard mode, with a trend indicating a decrease at 74.8 L/ha application volume compared to 37.4 L/ha.

3.5. Spatial variability in spray distribution

Spray distribution plots were generated to evaluate the positional effects of different operation modes on spray coverage within the simulated canopy structure (Figure 11). These plots revealed significant spatial variability in spray distribution across the seven predefined positions - center, southeast (SE), southwest (SW), south (S), northeast (NE), northwest (NW), and north (N) – for the three operation modes (standard, spinning, and fruit tree).

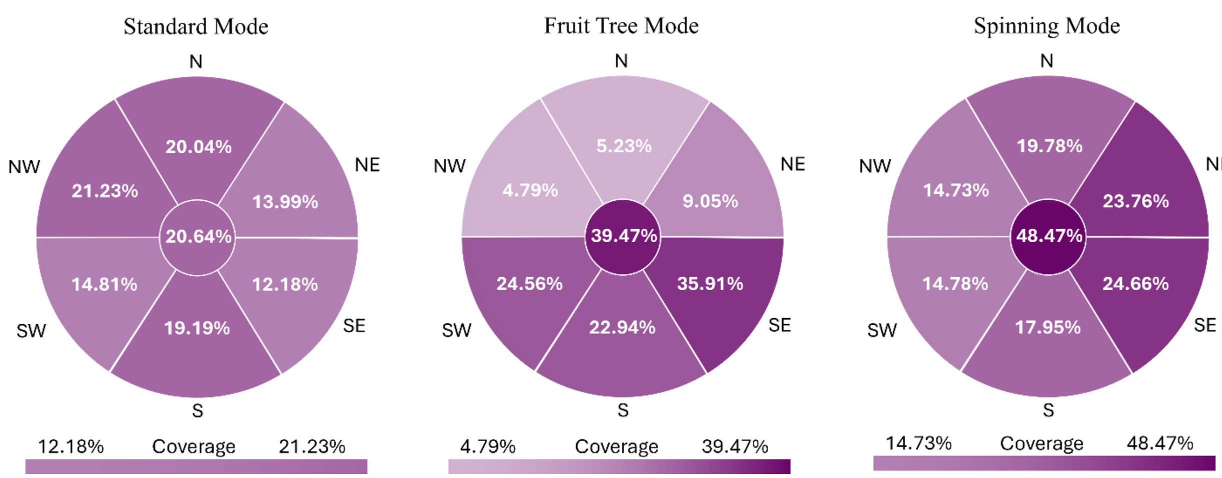

Figure 11. Spray distribution across different sampling locations within the canopy simulation structure for three operation modes: standard mode, spinning mode, and fruit tree mode. Sampling locations: SE: southeast, SW: southwest, S: south, NE: northeast, NW: northwest, and N: north. Darker shading indicates higher spray coverage.

The standard mode demonstrated the most uniform spray distribution across all sampling locations, despite delivering lower overall spray coverage compared to the other operation modes. Among the positions, the northwest recorded the highest spray coverage (21.23%), followed by the center (20.64%), north (20.04%), and south (19.19%) positions, which exhibited similar coverage levels. Peripheral positions, including southeast (12.18%), southwest (14.81%), and northeast (13.99%) showed slightly lower spray coverage.

The fruit tree mode exhibited the highest spatial variability in spray coverage among the three operation modes. The center and southeast positions recorded the highest spray coverage (39.47% and 35.91%, respectively), while peripheral positions such as north (5.23%), northeast (9.05%), and northwest (4.79%) received minimal coverage. The southwest (24.56%) and south (22.94%) position exhibited moderate spray coverage.

The spinning mode achieved the highest overall spray coverage with a relatively balanced distribution across the simulated canopy structure. The center position recorded the highest spray coverage (48.47%), followed by consistent coverage across peripheral positions, including the southeast (24.66%), northeast (23.76%), south (17.95%), southwest (14.78%), and northwest (14.73%).

4. DISCUSSION

This study evaluated the effects of drone operational parameters (operation mode, application volume, droplet size, and flight height) on spray coverage, droplet density, droplet diameter, and droplet size uniformity in fruit tree orchard simulations. The results highlight the significant main effects and two-way, three-way, and four-way interactions ($p \leq 0.05$) among these factors, emphasizing the importance of optimizing these parameters to enhance pesticide deposition efficiency, improve canopy coverage, and reduce chemical waste.

Among the operation parameters, the spinning mode emerged as the most effective, achieving the highest average spray coverage (20.81%) and droplet density (172.44 drops/cm^2), along with uniform droplet distribution, and balanced spatial variability. Under optimal conditions (74.8 L/ha application volume, 3 m flight height, and 300 μm droplet size), spinning mode achieved a maximum spray coverage of 37.80%. In peripheral positions, spray coverage ranged from 14.73% (northwest) to 24.66% (southeast), while central position reached 48.47% of coverage. In this mode, the drone combines spotting with rotational spraying. This rotary spraying mechanism disperses droplet uniformly, resulting in a well-distributed spray pattern across the simulated canopy structure (DJI, 2022; Shan et al., 2024b). These findings align with a prior study that highlights the advantages of rotational application in achieving improved spatial distribution due to their ability to generate consistent droplet patterns across varying angles (Byers et al., 2024).

The standard mode, while slightly less effective in terms of the overall coverage and density compared to spinning mode, provided the most uniform spatial distribution, with spray coverage ranging from 12.18% (southeast) to 21.23% (northwest). Under optimal conditions (74.8 L/ha application volume, 3 m flight height, and 150 μm droplet size), this mode achieved a maximum spray coverage of 37.80%. The forward movement of the drone in the standard mode extends the horizontal range of droplets, increasing coverage across a broader area (DJI, 2022; Shan et al., 2024b). In addition, its continuous flight path likely contributed to its uniform deposition, making it suitable for applications that require consistent coverage over large areas (Shan et al., 2024b). In contrast, the fruit tree mode exhibited the lowest coverage (24.52%) under optimal conditions (an application volume of 74.8 L/ha, a flight height of 5 m, and a droplet size of 300 μm), a significant spatial variability, with coverage concentrated at central (39.47%) and southeast (35.91%) positions of the simulated canopy structure and reduced coverage at peripheral locations, such as northwest (4.79%) and north (5.23%). This operation mode employs a spot spraying pattern, where the drone remains relatively stationary, spraying only while hovering over a target area, facilitating targeted droplet deposition in specific areas (Shan et al., 2024b). While this operation mode concentrates droplets in a specific spot, it limits horizontal coverage and is less effective for evenly distributing the spray over larger areas (DJI, 2022; Shan et al., 2024b). The rear placement of the drone's atomizers led to reduced spray deposition in the front part of the target area, contributing to the observed variability.

The influence of application volume and flight height were consistent across modes. Higher application volume (74.8 L/ha) significantly enhanced spray coverage and droplet density. For example, increasing the application volume from 37.4 L/ha to 74.8 L/ha improved droplet density from 114.00 to 146.35 drops/cm^2 on average. This trend can be attributed to the increased liquid available for deposition, which enhances coverage and droplet density (Paul et al., 2024; Yan et al., 2023). Lower flight height (3 m) produced significantly greater coverage and droplet density, likely due to reduced impact of drift, and evaporation (Byers et al., 2024; P. Chen et al., 2021).

The impact of droplet size was mode-dependent, reflecting the need for tailored parameter configurations. Smaller droplets (150 µm) enhanced coverage and droplet density in the standard and spinning modes, possibly due to their higher surface area-to-volume ratio, which improves contact with target surfaces (P. Chen et al., 2020; Shan et al., 2021). Conversely, larger droplets (300 µm) were more effective in the fruit tree mode, possibly due to the hovering mechanism allowing better deposition of heavier droplets with reduced drift potential. The hovering operation, combined with the vertical release of spray at fixed points, may have favored the gravitational settling of larger droplets, reducing lateral dispersion and enhancing localized deposition. These findings align with observations reported by (S. Chen et al., 2020), who demonstrated that increased droplet size significantly improved deposition rates and penetration while effectively reducing drift during drone spraying in rice canopies.

Droplet diameter (Dv0.1, Dv0.5, and Dv0.9) and RSF varied across modes, with standard mode producing the largest droplets (e.g., Dv0.9: 593.66 µm), which contributed to its higher RSF values and less uniform distribution. In contrast, the spinning and fruit tree modes generated smaller and more uniform droplets (e.g., RSF: 0.86-0.94), indicating improved deposition efficiency (Basílio et al., 2024; J. Chen et al., 2024; Mohanty & Raheman, 2024). Increasing application volume (74.8 L/ha) and droplet size (300 µm), and decreasing flight height (3 m) consistently enlarged droplet diameter, resulting in less uniform droplets (Silva et al., 2024). These findings reinforce the need to consider droplet uniformity when optimizing spray parameters for specific agricultural applications.

Overall, this study highlights that no single drone operation mode is universally superior. Instead, the selection of optimal parameters should be dictated by specific application goals, crop canopy structure, and environmental conditions. The spinning mode, with its rotational spray and superior coverage, is ideal for dense canopies requiring thorough coverage, using a 74.8 L/ha application volume, 3 m flight height, and 300 µm droplet size. The fruit tree mode offers advantages in droplet uniformity and targeted application in smaller orchards, using a 74.8 L/ha volume, 5 m flight height, and 300 µm droplets. While the standard mode's consistent spatial coverage is well-suited for achieving uniform coverage over large, open areas, particularly with a 74.8 L/ha application volume, 3 m flight height, and 150 µm droplet size.

These findings support the growing body of research advocating for data-driven parameter tuning in drone-based crop protection (García-Munguía et al., 2024b; Raj et al., 2024), reinforcing the potential of drones as adaptable tools in precision agriculture.

5. CONCLUSION

This study demonstrated the potential of optimizing drone spray parameters to enhance pest management in fruit tree orchards. By systematically evaluating the effects of operation mode, application volume, flight height, and droplet size on spray coverage, droplet density, droplet diameter, and droplet size uniformity, the findings highlight the importance of parameter-specific configurations in maximizing spray efficacy. Among the operation modes tested, the spinning mode emerged as the most versatile and effective, achieving superior spray coverage (up to 37.80%), high droplet density (198.91 drops/cm^2), uniform droplet distribution, and balanced spatial deposition. Its rotary application mechanism makes it ideal for dense canopies requiring thorough coverage. In contrast, the fruit tree mode demonstrated strong potential for localized deposition, particularly with larger droplets, making it a suitable option for precision applications in small orchards. Although the standard mode achieved the lowest overall coverage and density, it provided the most uniform spatial distribution, indicating its potential utility as scenarios requiring consistent deposition over large, open areas. The study also identified key parameter combinations critical for performance. Specifically, a higher application volume of 74.8 L/ha, a flight height of 3 m for spinning and standard modes (5 m for the fruit tree mode), and a droplet size of 150 µm for standard and spinning modes (300 µm for fruit tree mode) were optimal for maximizing coverage. These results provide a framework for developing tailored drone spraying strategies that improve coverage efficiency, minimize drift, and reduce chemical inputs. Although this study was conducted using simulated canopy structures, the observed trends align with reported field dynamics and offer a robust foundation for real-world applications. Future studies should focus on validating these configurations under field conditions. Emerging advances in drone technology, such as adaptive spray systems, hold significant promises for further enhancing precision, efficiency, and sustainability of pesticide applications in modern agriculture practices.

Chapter III

Evaluation of drone operational parameters for improved spray coverage and droplet distribution in a peach orchard

Abstract

Peach orchards face significant challenges in managing pests and diseases, which can reduce yield and fruit quality. While conventional air-blast sprayers have been widely used, they often result in excessive pesticide discharge, contributing to high costs and environmental contamination. Unmanned aerial vehicles (drones) have emerged as a promising alternative for pesticide application, offering improved precision and sustainability. This study evaluated the effects of different drone spraying treatments (fruit tree, spinning, and standard), canopy layers, and sampling locations on spray coverage, droplet density, droplet diameter, and droplet size uniformity in a peach orchard. Optimized operational parameters for application volume, flight height, and droplet size were used, and drone spraying results were compared with those of a conventional air-blast sprayer. The results demonstrated that the fruit tree treatment achieved the highest spray coverage (6.55%) and droplet density (90.09 drops/cm²), outperforming both the spinning (3.74% and 54.59 drops/cm²) and standard treatments (1.19% and 6.68 drops/cm²). The air-blast sprayer demonstrated superior overall spray coverage (58.77%) and droplet density (193.11 drops/cm²), but the drone treatments, particularly the fruit tree and spinning, exhibited potential for targeted applications with reduced chemical waste. Sampling location had significant effects on spray deposition, with the south-facing sections of trees receiving the highest droplet density in drone applications. Notably, canopy layer had no significant effect on spray deposition, suggesting efficient spray penetration due to drone-generated airflow. This study highlights the

potential of drones as a sustainable and efficient alternative to conventional sprayers, providing insights into future drone design optimization for improved orchard management.

1. INTRODUCTION

Peach (*Prunus persica* (L.) Batsch) is a deciduous fruit tree belonging to the Rosaceae family (subfamily Amygdaloideae) (Manganaris et al., 2022). In 2023, it was the sixth most-produced fruit worldwide (Manganaris et al., 2022; USDA, 2023). China led global production with 17,516,500 tons, followed by Spain (1,381,780 tons), Turkey (1,076,852 tons), Italy (1,033,840 tons), and the United States (U.S.) (665,910 tons) (*FAOSTAT*, 2025). Despite its economic and agricultural significance, U.S. peach production has declined by more than 30% over the past decade (*FAOSTAT*, 2023), with per capita consumption decreasing from 3.31 kg in 2012 to 1.97 kg in 2022 (Ritchie et al., 2023). One factor contributing to this decline is the high susceptibility of peaches to pests and diseases, which significantly reduce yield and fruit quality (Luo et al., 2022). For example, in Georgia U.S., peach diseases resulted in economic losses exceeding $5 million in 2018, with $3.9 million attributed to disease control costs (Brannen, 2018).

Pesticides application is essential for maintaining peach yield and quality (Meng et al., 2020). Conventional air-blast sprayers, widely used in peach orchards and other specialty crop production, have been a key tool in pest and disease management by ensuring efficient pesticide application (Boatwright et al., 2020). However, these sprayers present significant challenges, including excessive pesticide discharge, which increases costs and contributes to environmental contamination (Wei, Xue, et al., 2023).

Unmanned aerial vehicle (drones) have emerged as a promising alternative for pesticide application in orchards, offering advantages over air-blast sprayers in terms of efficiency, precision, and sustainability (Gao et al., 2020; García-Munguía et al., 2024a; Lopes et al., 2023;

Mahmud et al., 2021). Unlike conventional sprayers, drones enable targeted pesticide delivery, reducing chemical usage and minimizing human exposure to hazardous substances (Arakawa & Kamio, 2023; S. Guo et al., 2022; Meng et al., 2020; Yan et al., 2023). These advantages contribute to reduced pesticide waste, improved water conservation, time savings, and lower operational costs, making drones a sustainable and cost-effective solution for modern orchard management (Sahni et al., 2024; Wei, Li, et al., 2023). Studies have demonstrated that drones can achieve comparable pesticide application efficacy to air-blast and high-pressure sprayers, as reported by (Arakawa & Kamio, 2023). Similarly, (Li et al., 2021) found that while ground sprayers provided higher overall coverage on almond trees, drones achieved superior coverage in the upper canopy, highlighting their potential as a complementary approach to traditional ground-based application methods.

Effective pesticide application depends on achieving optimal droplet deposition (S. Guo et al., 2019; Muhammad et al., 2019; Srinivasarao et al., 2021). For efficient pest control, droplets must reach and penetrate the leaf surface (Song et al., 2022). However, a significant proportion of sprayed droplets often fail to reach the target, resulting in pesticide waste, reduced effectiveness, and increased environmental contamination risks (S. Guo et al., 2019; Meng et al., 2020). Several factors influence spray performance, including flight height (Qin et al., 2018; Tang et al., 2018), spray volume (G. Wang, Lan, Qi, et al., 2019), and droplet size (S. Chen et al., 2020). Recent advancements in drone spraying technology have introduced operation modes specifically designed for fruit trees, although these modes remain largely unexplored (García-Munguía et al., 2024a; Shan et al., 2024b). Achieving uniform spray distribution over tree canopies continues to be challenging, with spray performance in the lower layers of the canopy often being suboptimal

(Tang et al., 2018). Therefore, optimizing drone operational parameters is essential for achieving uniform and effective pesticide deposition.

This study aimed to evaluate the effects of optimized drone operational parameters for application volume, flight height, and droplet size (as determined in Chapter II) across three operation modes (fruit tree, spinning, and standard) on spray coverage, droplet density, droplet diameter, and droplet size uniformity in a peach orchard. The drone performance was compared to that of a conventional air-blast sprayer. Additionally, spatial variability in spray distribution was assessed by analyzing spray coverage and droplet density across different canopy layers (upper, middle, and lower) and sampling locations (center, north, east, south, and west) within peach trees.

2. MATERIALS AND METHODS

2.1. Experimental site

Field experiments were conducted at the Chilton Horticulture Substation in Clanton, AL (32°54'45"N, 86°40'06"W) on September 10, 2024. The study area covered 0.42 ha, with a plant-to-plant and row-to-row spacing of 5 m and 7 m, respectively. The selected trees had an average height of 2.6 m and a canopy width of 6 m.

Meteorological data, including wind speed (m/s), temperature (°C), and relative humidity (%), were recorded every 10 s using a Kestrel 5500 weather meter (Kestrel Instruments, Boothwyn, PA, USA), mounted on a tripod at a height of 1.8 m. Weather conditions were averaged across all treatments and are summarized in Table 9.

Table 9. Meteorological conditions during the application day.

Parameter	10-September
Temperature (°C)	25.55 ± 1.03[a]
Relative humidity (%)	69.41 ± 6.22
Wind speed (m/s)	0.76 ± 0.54

[a] Results are presented as mean ± standard error.

All experiments were performed under wind speeds below 2 m/s and wind angles within ± 15°, in accordance with the ASAE S386.2 standard (American Society of Agricultural Engineers, 1988).

2.2. Spray equipment

2.2.1. Drone sprayer

The drone sprayer used in this study was the DJI Agras T40 (SZ DJI Technology Co., Shenzhen, China), an eight-motor coaxial multi-rotor drone (Figure 12). The drone weighs 50 kg, has a 40 L tank capacity, and dimensions of 2.8 m × 3.15 m × 0.78 m (L × W × H). It can achieve a maximum speed of 36 km/h and provides an effective spray width of 11 m when flying at a speed of 7 m/s and an altitude of 2.5 m. The DJI T40 is equipped with a dual-atomized spray system that produces droplets ranging from 50 to 500 μm, with each nozzle supporting a maximum flow rate of 6 L/min (DJI, 2022).

Figure 12. DJI Agras T40 drone sprayer used in the spraying experiments.

For enhanced precision, the DJI Agras T40 was paired with a GNSS mobile base station (Model D-RTK 2), achieving horizontal and vertical accuracies within ±10 cm. The drone was also equipped with omnidirectional radar and a terrain-following system, enabling operation on inclines of up to 30°. Flight control and spray management were conducted using the DJI Agras intelligent remote controller, which is integrated with flight planning software. Orthomosaics of the experimental area were generated using DJI Terra software (SZ DJI Technology Co., Shenzhen, China) ensuring precise flight path planning.

The drone was operated in three operation modes (standard, fruit tree, and spinning) using optimized parameters for application volume, flight height, and droplet size, as determined in Chapter II. In standard mode, the drone followed a continuous flight path, applying the spray solution at a volume rate of 74.8 L/ha with a droplet size of 150 µm, and a flight height of 3 m. In fruit tree mode, the drone hovered at the center of each target area, activated its nozzles, and sprayed the solution at a volume rate of 74.8 L/ha with a droplet size of 300 µm, and a flight height of 5 m before proceeding to the next target. The spinning mode involved the drone hovering at the center of the target area, rotating around its axis while spraying the solution at a volume rate of 74.8 L/ha with a droplet size of 300 µm, and a flight height of 3 m before moving to the next target.

2.2.2. Air-blast sprayer

The conventional sprayer used in this study was the Jacto Arbus 2000 air-blast sprayer. It has a 2000 L tank capacity, a maximum flow rate of 75 L/min, and an operational speed of up to 6 km/h (Jacto Inc, 2011). The air-blast sprayer weighs 700 kg and has dimensions of 4.45 m ×1.75 m ×1.85 m (L × W × H). In this spraying treatment, the solution was applied at a volume rate of 467.7 L/ha at 5 km/h along a continuous path. The sprayer initially targeted the left side of the selected trees at a constant rate and then returned along an adjacent path to treat the right side of the same trees.

2.3. Experimental design

A three-factorial experimental design with four replicates was used to evaluate the effects of spraying treatment (fruit tree, spinning, standard, and air-blast sprayer), canopy layer (upper, middle, and lower), and sampling location (center, north, east, south, and west) on spray coverage, droplet density, droplet diameter, and droplet size uniformity.

Four peach trees of similar size and canopy shape were selected for each spraying treatment, with each tree serving as a replication. The canopy of each tree was vertically divided into three layers: upper (2.6 m), middle (1.8 m), and lower (1 m) (Figure 13a). Within each layer, sampling was conducted at five locations: center, north, east, south, and west sides of the canopy (Figure 13b). A leaf was randomly selected within each sampling zone, and Kromekote White Paper (KWP) cards (The Paper Mill Store, Neenah, WI, USA) were strategically placed, resulting in a total of 15 KWP cards per tree. A buffer zone of at least 10 m was maintained between replications to minimize spray drift effects (Figure 13c). This layout ensured accurate and independent spray deposition measurements.

Spray deposition performance was evaluated using a water-based solution containing 20 mL/L of Vision Pink™ dye (GarrCo Products, Converse, IN, USA).

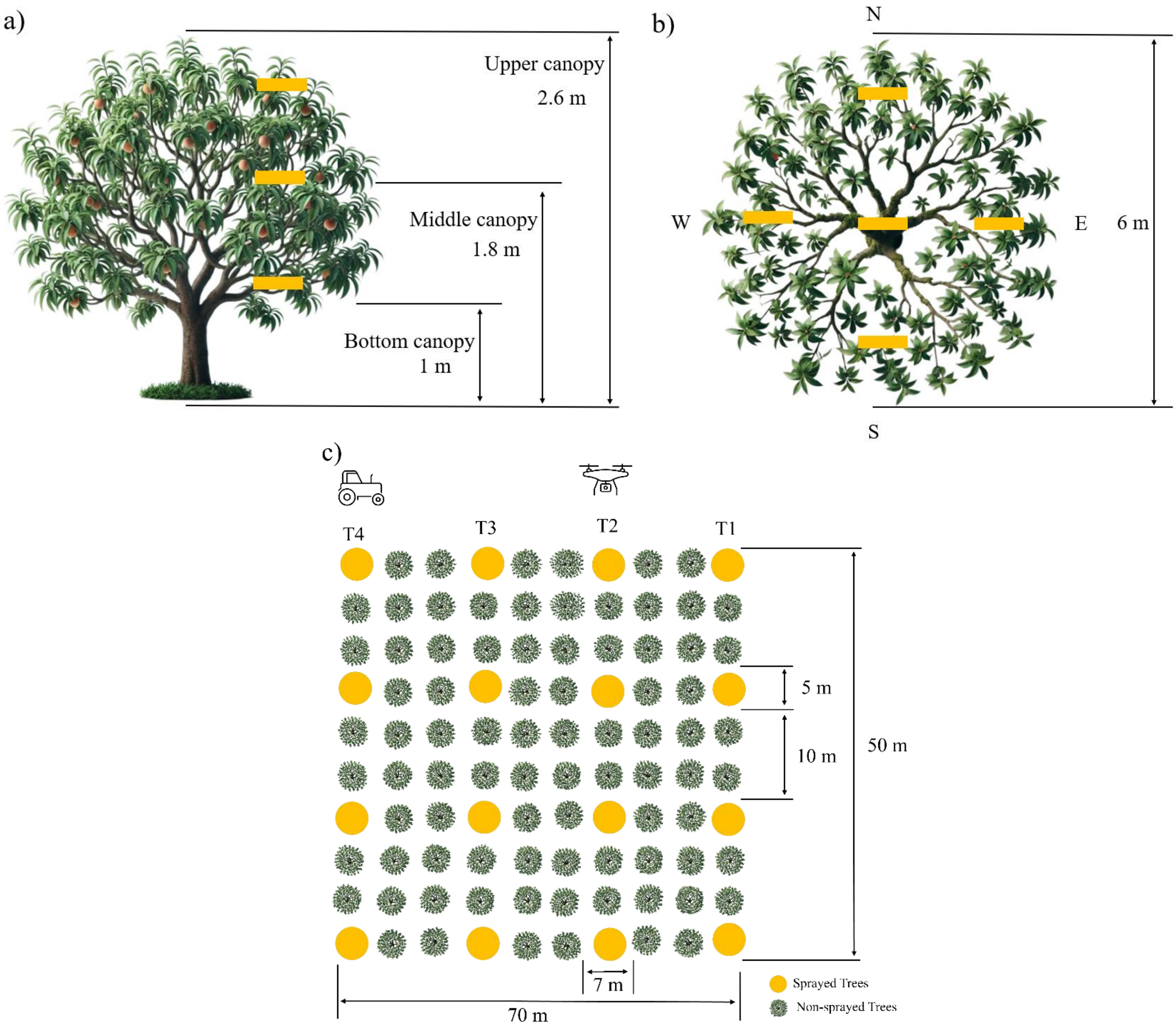

Figure 13. Experimental layout and Kromekote White Paper (KWP) card placement (yellow) within the peach tree canopy. (a) Side view illustrating canopy layers (upper, middle, and lower). b) Top view showing KWP card placement at five canopy locations (center, north, east, south, and west). c) Experimental layout illustrating selected trees and buffer zones. Abbreviations: N – north, S – south, W – west, E – east, T1 – fruit tree spraying treatment, T2 – spinning spraying treatment, T3 – standard spraying treatment, and T4 – air-blast spraying treatment.

2.4. Data collection and processing

After the spraying application, KWP cards were collected from the trees, stored in pre-labeled adhesive note blocks, and sealed in plastic bags with silica pouches to prevent moisture contamination. The KWP cards were scanned at a resolution of 1200 dpi using an Epson Perfection V39II flatbed scanner (Epson America Inc., Long Beach, CA, USA). The scanned images were processed using AccuStain software (Version 0.32, developed by Matt Gill, University of Illinois at Urbana-Champaign, USA), using default settings for cast-coat papers to calculate key spray deposition metrics. Spray coverage (%) was calculated as the ratio of the spray deposit area (stain-covered area) to the total area analyzed on the KWP cards (Gill, 2024). Droplet density (drops/cm^2) was determined by counting the number of droplets deposited per unit area on the cards. Droplet diameter (μm) was analyzed at three points: Dv0.1, the diameter at which 10% of the spray volume consists of droplets smaller than Dv0.1; Dv0.5 (volume median diameter), the midpoint where 50% of the spray volume is composed of droplets smaller than Dv0.5, and 50% of droplets larger than Dv0.5; and Dv0.9, the diameter at which 90% of the spray volume consists of droplets smaller than Dv0.9. Droplet size uniformity was determined using the relative span factor (RSF), calculated according to equation (1) (Gill, 2024) .

$$RSF = \frac{Dv0.9 - Dv0.1}{Dv0.5} \qquad \text{Equation (2)}$$

2.5. Statistical analysis

Data was analyzed using a generalized linear mixed model, implemented with the PROC GLIMMIX procedure in SAS software (version 9.04.01M7P08062020). Drone spraying treatment, canopy layer, sampling location, and their interactions were used as fixed effects on spray coverage, droplet density, droplet size uniformity (RSF), and droplet diameter (Dv0.1, Dv0.5, and Dv0.9). Similarly, spraying treatment (drone and air-blast), canopy layer, sampling location, and their interactions were considered fixed effects on spray coverage and droplet density. An analysis of variance was conducted to determine the significance of the main effects and their interactions. When the analysis of variance indicated significant effects ($p \leq 0.05$), least-square mean comparisons were performed using Tukey's test with an adjusted *p*-value of 0.05. Additionally, an orthogonal contrast analysis was performed to statistically compare the performance of the drone spraying treatments with the air-blast sprayer.

An overspray index was calculated to compare spray coverage across treatments, following the method described by Y. Chen et al. (2013). Overspray was defined as any instance where spray coverage exceeded 30%. The index was calculated using the following equation (2):

$$I_0 = \frac{C-30}{100-30} \qquad \text{Equation (3)}$$

where I_0 represents the overspray index and C is the spray coverage observed on a given card. This index standardizes coverage relative to the 30% threshold, resulting in values that range from −0.4 (corresponding to 0% coverage) to 1.0 (corresponding to 100% coverage).

3. Results

3.1. Spray coverage and droplet density

Drone spraying treatments, sampling location, and their interaction had statistically significant effects on spray coverage and droplet density ($p \leq 0.01$). However, canopy layer and its interaction with drone spraying treatments and sampling location did not significantly affect spray coverage and droplet density ($p > 0.05$). Among the drone spraying treatments, the fruit tree achieved the highest spray coverage at 6.55%, significantly outperforming the spinning (3.74%) and the standard (1.19%) (Figure 14a).

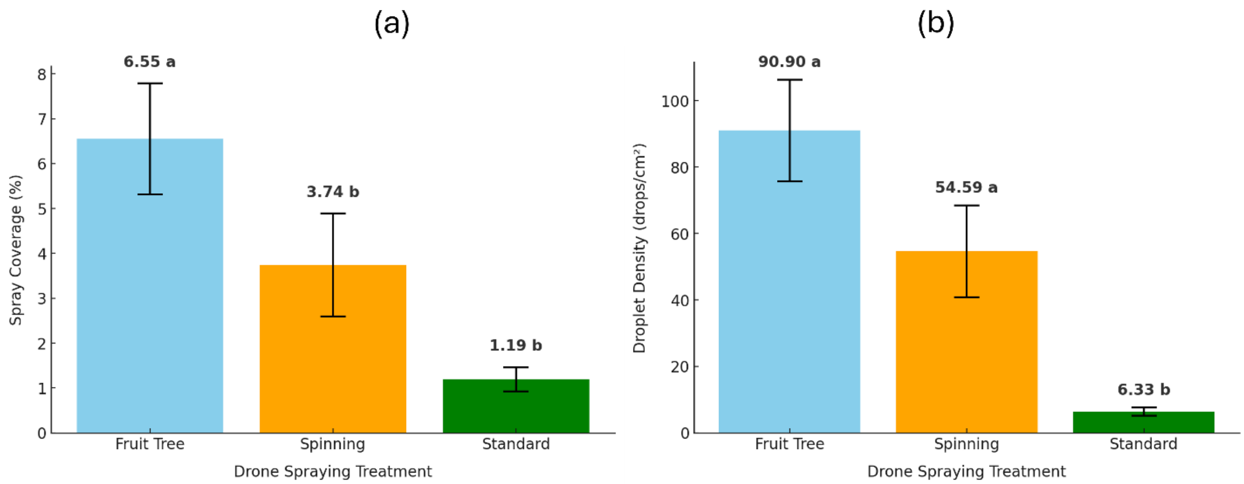

Figure 14. Effect of drone spraying treatments on (a) spray coverage and (b) droplet density. Error bars represent standard deviations. Similar lowercase letters indicate no significant differences among drone spraying treatments ($p > 0.05$), as determined by Tukey's test.

3.2. Droplet diameter (Dv01, Dv0.5, Dv0.9) and relative span factor (RSF)

The main effect of drone spraying treatment was statistically significant for Dv0.5 ($p \leq 0.01$), Dv0.9 ($p \leq 0.05$), and RSF ($p \leq 0.01$). Additionally, sampling location significantly influenced droplet diameter (Dv01, Dv0.5, Dv0.9) ($p \leq 0.01$), while the interaction between drone spraying treatments and sampling location was significant only for Dv0.1 ($p \leq 0.05$). Canopy layer and its interaction with drone spraying treatments and sampling location did not significantly affect droplet diameter (Dv01, Dv0.5, Dv0.9) and RSF ($p > 0.05$).

For droplet diameter (Figure 15a), no significant differences were observed among the drone spraying treatments for Dv0.1. However, for Dv0.5, both the fruit tree and spinning treatments produced the largest droplets (183.19 µm and 186.49 µm, respectively). In contrast, the standard treatment generated significantly smaller droplets, with an average Dv0.5 of 143.74 µm. Similarly, for Dv0.9, there were no significant difference between the fruit tree treatment (264.29 µm) and the spinning treatment (264.04 µm), while the standard treatment produced the significantly smaller droplets (220.33 µm).

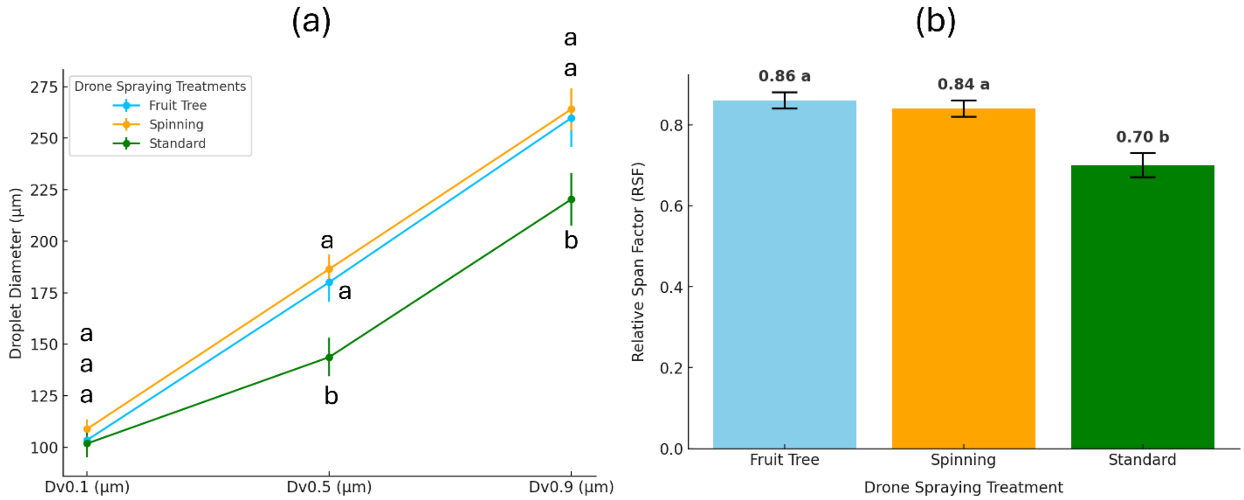

Figure 15. Effect of drone spraying treatments on (a) droplet diameter and (b) relative span factor (RSF). Similar lowercase letters indicate no significant differences among drone spraying treatments at each droplet diameter or RSF value ($p > 0.05$), as determined by Tukey's test. Error bars represent standard deviations.

Regarding droplet size uniformity, the RSF values for the fruit tree treatment (0.86) and spinning treatment (0.84) were not significantly different (Figure 15b). However, the standard treatment had a significantly lower RSF value of 0.70.

3.3. Spatial variability in spray distribution

Table 10 presents the effects of sampling location (center, east, west, south, and north) under different drone spray treatments on spray coverage within the peach tree canopy.

Table 10. Interaction effect of drone spraying treatment and sampling location on spray coverage within the peach tree canopy.

Drone spraying treatment	Sampling location	Spray coverage (%)
Fruit tree	South	16.52 a
	East	8.00 b
	Center	4.95 bc
	West	2.68 c
	North	0.53 c
Spinning	South	11.86 a
	East	2.71 b
	Center	3.85 b
	West	0.10 b

	North	0.17 b
Standard	South	1.20 a
	East	1.04 a
	Center	0.86 a
	West	1.11 a
	North	2.07 a
Drone spraying treatment *vs* sampling location *p*-value		**

Similar lowercase letters indicate no significant differences in spray coverage between the sampling location within each drone spraying treatment, as determined by Tukey's test. Level of significance (*p*-value): **, significant at $p \leq 0.01$.

For the fruit tree treatment, the highest spray coverage was observed in the south sampling location, with a coverage of 16.52%, followed by the east (8.00%), center (4.95%), west (2.68%), and north (0.53%) locations, which showed the lowest coverage. In the spinning treatment, the south location again exhibited the highest spray coverage (11.86%), which was significantly higher than the east (2.71%), center (3.85%), west (0.10%), and north (0.17%) locations. No significant differences were observed among the spray coverage at the east, center, west, and north locations. The standard treatment showed a uniform distribution of spray coverage across all sampling locations, with no significant differences in spray coverage between the locations. The south location had the highest spray coverage (1.20%), followed closely by the west (1.11%), north (2.07%), east (1.04%), and center (0.86%).

Spray distribution plots were generated to evaluate the positional effects of sampling location (center, east, west, south, and north) under the different drone spray treatments on droplet density (Figure 16) within the peach tree canopy.

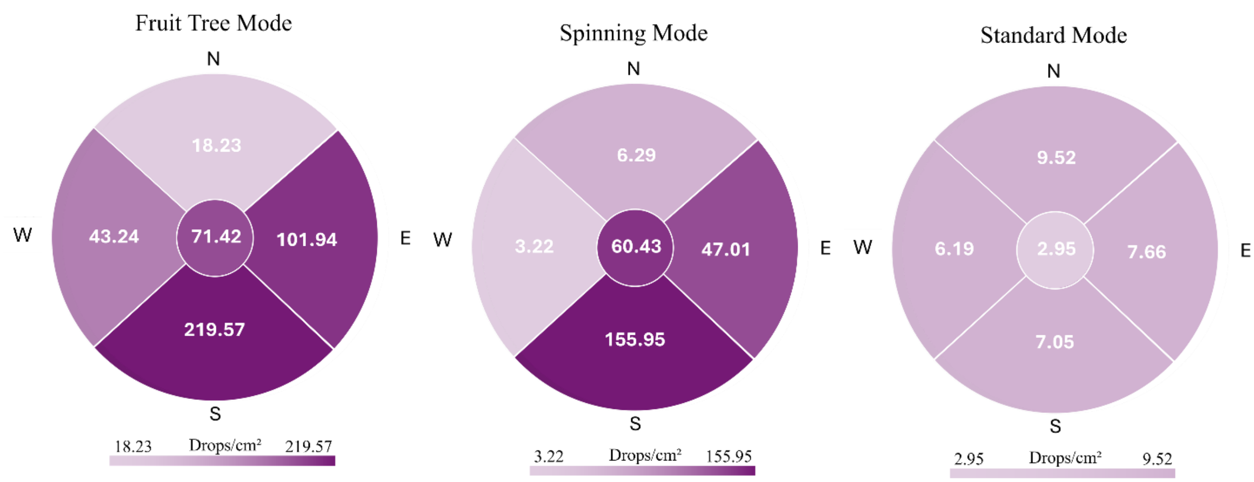

Figure 16. Droplet density distribution across different sampling locations within the peach tree canopy for three drone spraying treatments: standard, spinning, and fruit tree. Sampling locations: E: east, W: west, S: south, and N: north. Darker shading indicates higher droplet densities.

The fruit tree treatment demonstrated the highest overall droplet density, with the south position exhibiting the greatest droplet density (219.57 drops/cm²), followed by the east (101.94 drops/cm²) and center (71.42 drops/cm²) locations. Lower droplet densities were observed in the west (43.24 drops/cm²) and north (18.23 drops/cm²) locations.

The spinning treatment resulted in moderate droplet densities, with the south location again recording the highest deposition (155.95 drops/cm²), followed by the center (60.43 drops/cm²) and east (47.01 drops/cm²) locations. The lowest droplet densities were observed in the north (6.29 drops/cm²) and west (3.22 drops/cm²) locations.

The standard treatment produced the lowest overall droplet density but exhibited a more uniform distribution. The north and east locations had slightly higher droplet densities (9.52 drops/cm² and 7.66 drops/cm², respectively), whereas the south, west, and center locations recorded lower densities (7.05 drops/cm², 6.19 drops/cm², and 2.95 drops/cm², respectively).

3.4. Drone *vs* air-blast sprayer

Spraying treatments (drone and air-blast sprayer), sampling location, and their interactions had statistically significant effects on droplet density ($p \leq 0.01$). However, canopy layer and its interaction with spraying treatment and sampling location did not significantly affect droplet density ($p > 0.05$).

Figure 17(a) illustrates the droplet density obtained from the air-blast sprayer and drone spraying treatments (fruit tree, spinning, and standard). The air-blast sprayer exhibited the highest droplet density, averaging 193.11 drops/cm², with values ranging from 0.27 to 490.16 drops/cm². The fruit tree treatment recorded the second-highest droplet density, averaging 90.90 drops/cm², with a range of 0 to 456.98 drops/cm², followed by the spinning treatment, which had an average of 54.59 drops/cm² and ranged from 0.19 to 421.82 drops/cm². The standard treatment resulted in the lowest droplet density, averaging 6.33 drops/cm², with values ranging from 0 to 38.98 drops/cm².

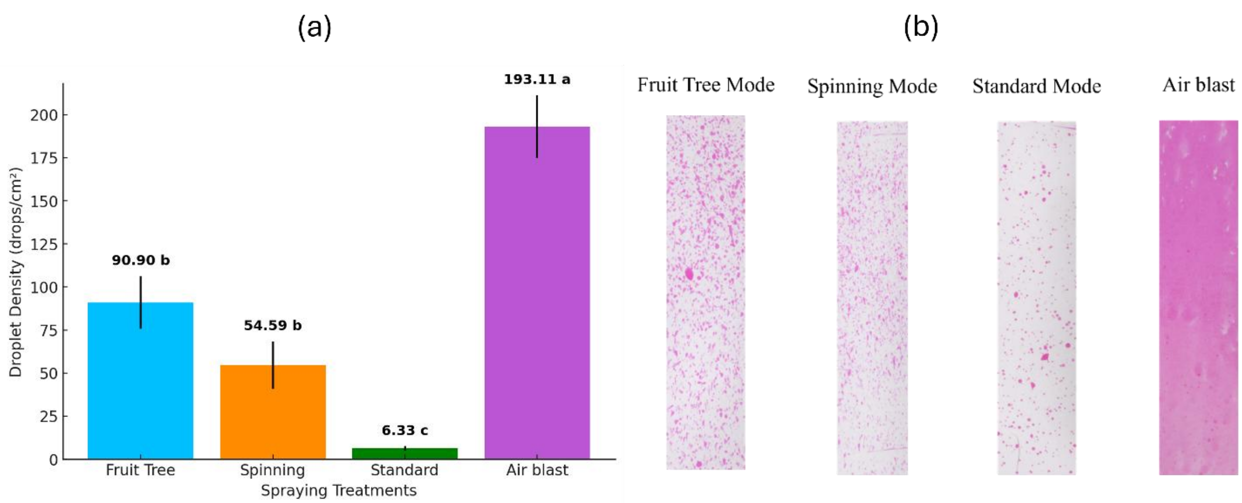

Figure 17. (a) Droplet density distribution and (b) representative images of Kromekote White Paper (KWP) cards showing spray coverage patterns for drone spraying treatments (fruit tree, spinning, and standard) and a conventional air-blast sprayer. Box plots represent the distribution of droplet density, with the median represented by the horizontal line within each box, and whiskers indicating the data range.

Spraying treatments (drone and air-blast sprayer), sampling location, and canopy layer had statistically significant effects on spray coverage ($p \leq 0.01$). Additionally, the interactions between spraying treatments and sampling location, as well as between spraying treatments and canopy layer, significantly affected spray coverage ($p \leq 0.01$). Figure 6b illustrates the spray coverage patterns on KWP cards for each spraying treatment. The air-blast sprayer demonstrated the highest coverage (58.77 %), with a dense and uniform distribution of spray droplets across the KWP card surface. The fruit tree treatment exhibited substantial coverage (6.55 %), though slightly less uniform than the air-blast treatment, with well-distributed droplets across the card. The spinning treatment resulted in moderate spray coverage (3.74 %), with noticeable gaps and a more dispersed droplet pattern. In contrast, the standard treatment displayed the lowest coverage (1.19 %), with sparse droplet deposition and inconsistent distribution.

The bar graph (Fig 18) presents the mean overspray index for the three drone operation modes in comparison to the air-blast sprayer. The air-blast treatment had the highest overspray index at 0.41, which was significantly greater than all drone-based treatments. Among the drone modes, there were no statistically significant differences in overspray index. The Fruit Tree mode had a mean overspray index of –0.33, the Spinning mode averaged –0.38, and the Standard mode achieved the lowest value at –0.41.

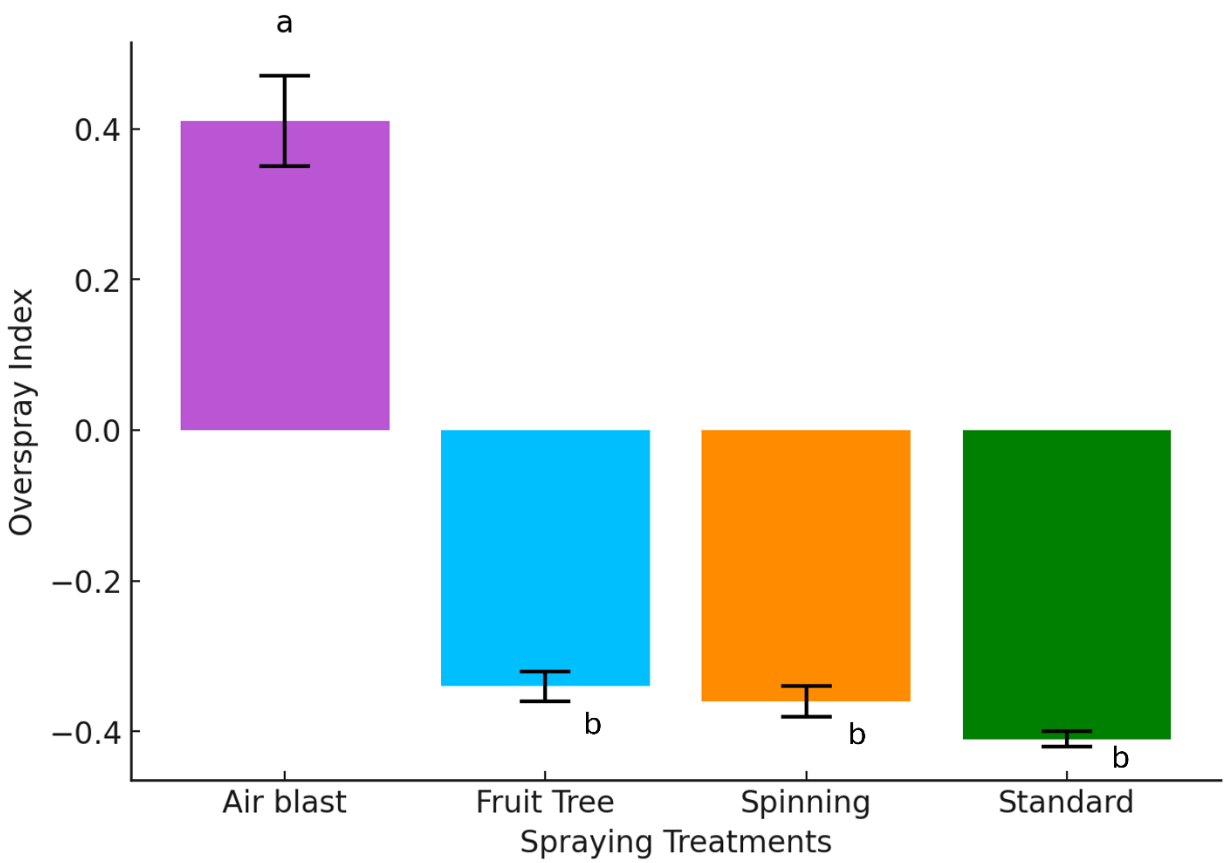

Figure 18. Bar graph comparing the overspray index between drone operation modes (fruit tree, spinning, and standard) and a convention air-blast sprayer. Similar lowercase letters indicate no significant differences among treatments ($p > 0.05$), as determined by Tukey's test. Error bars represent standard error.

A contrast analysis was performed to compare spray coverage between each drone spraying treatments and the conventional air blast sprayer (Table 11). The results revealed a significant difference ($p < 0.0001$) between the air-blast sprayer and all three drone spraying treatments.

Table 11. Contrast analysis between drone spraying treatments and the conventional air-blast sprayer.

Treatment	F value	*p*-value
Air blast *vs* Fruit tree	52.22	<0.0001
Air blast *vs* Spinning	55.04	<0.0001
Air blast *vs* Standard	57.58	<0.0001

4. DISCUSSION

The results of this study provide insights into the performance of different drone spraying treatments compared to conventional air-blast sprayers in peach orchards. Significant differences were observed in spray coverage, droplet density, droplet diameter, and droplet size uniformity across the different drone spraying treatments and sampling locations. However, canopy layer had no significant effect on spray deposition parameters, suggesting that the downwash airflow generated by the drone rotors may have facilitated spray penetration through the canopy (Q. Guo et al., 2020). This indicates that drones could provide efficient pesticide application across the vertical tree structure.

Among the drone spraying treatments, the fruit tree was the most efficient, achieving the highest spray coverage (6.55 %) and droplet density (90.09 drops/cm²), followed by the spinning (3.74% coverage and 54.59 drops/cm²) and the standard (1.19% coverage and 6.68 drops/cm²). These results indicate that the fruit tree treatment, which involves hovering over the target area, facilitates more efficient and targeted spray application, with higher spray coverage and droplet density compared to the other two drone spraying treatments. This prolonged time over the target, combined with the propeller's airflow, may enhanced canopy penetration (Q. Guo et al., 2020; Li et al., 2021; Shan et al., 2024b). However, the fruit tree treatment exhibited high spatial variability, primarily due to the rear placement of atomizers (DJI, 2022), which resulted in significantly higher spray deposits in the south (219.57 drops/cm²), east (101.94 drops/cm²), and center (71.42 drops/cm²) regions of the canopy compared to other directions.

The spinning treatment provided moderately higher coverage and droplet density than the standard treatment. These results are consistent with Arakawa & Kamio (2023), who demonstrated that the spinning spot spray mode outperformed continuous straight-flight spraying. In addition, the spinning treatment, while producing lower droplet densities overall compared to fruit tree treatment, still demonstrated a higher droplet density in the south location (155.95 drops/cm²) compared to other locations.

The shorter time over the target when using the standard treatment likely led to reduced spray coverage compared to the other treatments, which use a spot-spray system that extends flight time and increases time over the target (Arakawa & Kamio, 2023). Interestingly, this treatment achieved the most uniform spray application, with minimal spatial variability across all sampling locations. This uniformity is likely a result of its continuous straight flight path, which produces a forward momentum that evenly distributes droplets. However, its overall droplet density was much lower compared to the fruit tree and spinning treatment, indicating its less effective spray applications. The standard treatment may therefore be better suited for large-scale applications where spray uniformity is prioritized over higher coverage or penetration (Shan et al., 2024b).

The drone spraying treatments also significantly influenced droplet diameter, with the fruit tree and spinning treatments producing larger droplets (183.19 µm and 186.49 µm, respectively) compared to the standard treatment (143.74 µm). Larger droplets are generally more effective in reducing drift and ensuring better coverage on the target surface, which is essential for maximizing pest control while minimizing environmental contamination (Privitera et al., 2023; Srinivasarao et al., 2021). These results suggest that the fruit tree and spinning treatments, with their larger droplet sizes, may offer improved control of pesticide application over the standard treatment, which produced finer droplets that are more susceptible to drift and evaporation (Nogueira Martins et al., 2021; Privitera et al., 2023). Droplet size uniformity, measured using the RSF, also varied across the treatments. Both the fruit tree and spinning treatments exhibited similar RSF values (0.86 and 0.84, respectively), while the standard treatment had a significantly lower RSF (0.70), suggesting less variability in droplet size, which may suggest a improve in the consistency of pesticide deposition (Basílio et al., 2024; Mohanty & Raheman, 2024).

In comparison with the conventional air-blast sprayer, the drone spraying treatments showed significant differences in spray coverage and droplet density, with all drone treatments performing less effectively than the air-blast sprayer in terms of coverage and density. The air-blast sprayer, known for its high-volume rate application (467.7 L/ha), produced the highest droplet density and spray coverage, achieving a dense and uniform distribution across the target area, however the air-blast also demonstrated substantial overspray compared to all drone modes, consistently achieving a higher coverage than the 30% threshold. These results are consistent with Li et al. (2021), who reported similar differences between drone and conventional air-blast spraying methods. However, the drone spraying treatments, known for their low-volume rate application (74.8 L/ha), still demonstrated promising potential, especially the fruit tree and spinning treatments, which demonstrated high droplet density and coverage compared to the standard treatment. While higher droplet densities are generally associated with improved pest control effectiveness (Zhu et al., 2011), it is crucial to consider the recommended droplet density for specific pesticide applications. For example, pre-emergence herbicides and insecticides require 20-30 drops/cm^2, contact post-emergence herbicides require 30-40 drops/cm^2, and fungicides require 40-70 drops/cm^2 (Ghafoor et al., 2022; G. Wang, Lan, Yuan, et al., 2019; Zhu et al., 2011). The fruit tree and spinning treatments align well with these recommendations, making them optimal choices for such applications, whereas the standard treatments fall below the minimum requirement for pre-emergence herbicides and insecticides, limiting its practical use. In contrast, the air-blast sprayer exceeded the recommended droplet density for all pesticide types, which may result in excessive chemical usage and potential wastage. Therefore, the significant differences between drone spraying treatments and the air-blast sprayer highlight the potential for drones to serve as an efficient and more environmentally sustainable alternative (Jiang et al., 2022).

5. CONCLUSION

This study comprehensively evaluated the effects of different drone spraying treatments (fruit tree, spinning, and standard), canopy layers, and sampling locations on spray coverage, droplet density, droplet diameter, and droplet size uniformity, using optimized operational parameters for application volume, flight height, and droplet size in a peach orchard. Additionally, the results obtained by drone spraying treatments were compared to that of a conventional air-blast sprayer, focusing on spray coverage and droplet density. The results demonstrated that drone spraying treatments significantly influenced spray coverage and droplet density, with the fruit tree treatment achieving the highest spray deposition among the drone treatments. However, the air-blast sprayer exhibited the highest overall spray coverage (58.77 %) and droplet density (193.11 drops/cm^2), emphasizing its efficiency in delivering uniform spray applications but using high-volume applications. The spinning treatment provided moderate spray coverage (3.74 %) and droplet density (54.59 drops/cm^2), while the standard treatment was the least effective in all measured parameters, but excelled in spatial uniformity, making it suitable for large-scale applications prioritizing even spray distribution. A key finding of this study was that canopy layer had no significant effect on spray deposition, suggesting that the downward airflow generated by the drone rotors facilitated spray penetration across the canopy. Additionally, significant interactions between spraying treatments and sampling locations indicated that spatial variability plays a crucial role in spray deposition, with the south-facing sections of trees receiving the highest droplet density in drone applications. While drones did not surpass air-blast sprayers in overall spray deposition, the fruit tree and spinning treatments demonstrated potential as a viable alternative for applications requiring specific droplet density thresholds, such as fungicides and herbicides, offering precise and targeted application with reduced chemical waste. The excessive chemical usage of the air-blast sprayer raises concerns about wastage and environmental impact, especially given that it exceeded recommended droplet densities for pesticide applications, which could result in unnecessary chemical runoff and waste. These findings contribute to the growing body of research on drone-based precision agriculture, highlighting their potential role in sustainable and efficient orchard management. Future research should focus on optimizing drone designs, such as atomizer placement, to minimize spatial variability and enhance spray efficiency. Additionally, further field trials across diverse crops and environmental conditions are necessary to validate these findings and refine application protocols for broader agricultural use, particularly in applications that prioritize more targeted chemical use with minimal waste.

Chapter 4

Conclusion

This study highlights the potential of unmanned aerial vehicles as a transformative tool in modern pesticide application, offering a sustainable and precise alternative to conventional methods. Through systematic evaluation of drone operational parameters, including application volume, flight height, droplet size, and operation mode, this research demonstrated that spray performance can be significantly improved by optimizing these parameters.

In simulated orchard trials, the spinning mode of the DJI Agras T40 achieved the highest spray coverage and droplet density, while the standard mode ensured the most uniform spatial distribution. In field trials within a peach orchard, the fruit tree mode outperformed other drone modes in both spray coverage and droplet deposition, although conventional air-blast sprayers still delivered the highest absolute coverage. Notably, drone applications showed greater precision, reduced water waste, and effective canopy penetration, with no significant differences in deposition across canopy layers, likely due to the rotor-induced downwash airflow.

While traditional sprayers remain effective, particularly in achieving high-volume coverage, their efficiency comes at the cost of over spraying and environmental impact. In contrast, drone spraying treatments, especially the fruit tree and spinning modes, demonstrated considerable promise for targeted applications. These findings emphasize the importance of selecting operation modes and configurations based on crop type, canopy structure, management priorities and environmental conditions.

Altogether, this research supports the integration of drones into orchard pest management programs and provides insights into optimizing drone based spray systems. Future work should explore the economic viability of drone adoption, long-term pest control efficacy, and broader applications across diverse orchard systems. With further technological refinement and field validation, UAVs can play a central role in advancing precision agriculture and reducing the environmental footprint of crop protection practices.

Chapter 5

References

AgEagle. (2025). https://ageagle.com/drones/ebee-x/

American Society of Agricultural Engineers. (1988). *Calibration and Distribution Pattern Testing of Agricultural Aerial Application Equipment*. 1-. https://doi.org/10.13031/S2000.2013

Anthony, B. M., & Minas, I. S. (2022). Redefining the impact of preharvest factors on peach fruit quality development and metabolism: A review. *Scientia Horticulturae*, *297*. https://doi.org/10.1016/j.scienta.2022.110919

Arakawa, T., & Kamio, S. (2023). Control Efficacy of UAV-Based Ultra-Low-Volume Application of Pesticide in Chestnut Orchards. *Plants*, *12*(14). https://doi.org/10.3390/plants12142597

Basílio, S., Furtado Júnior, M. R., de Alvarenga, C. B., Vitória, E. L. da, Vargas, B. C., Privitera, S., Caruso, L., Cerruto, E., & Manetto, G. (2024). Effect of Adjuvants on Physical–Chemical Properties, Droplet Size, and Drift Reduction Potential. *Agriculture (Switzerland)*, *14*(12). https://doi.org/10.3390/AGRICULTURE14122271

Benos, L., Kateris, D., Tagarakis, A. C., & Bochtis, D. (2023). Developments in the era of unmanned aerial systems. *Unmanned Aerial Systems in Agriculture: Eyes Above Fields*, 3–24. https://doi.org/10.1016/B978-0-323-91940-1.00001-3

Berger-Neto, A., Jaccoud-Filho, D. de S., Wutzki, C. R., Tullio, H. E., Pierre, M. L. C., Manfron, F., & Justino, A. (2017). Effect of spray droplet size, spray volume and fungicide on the control of white mold in soybeans. *Crop Protection*, *92*, 190–197. https://doi.org/10.1016/j.cropro.2016.10.016

Boatwright, H., Zhu, H., Clark, A., & Schnabel, G. (2020). Evaluation of the intelligent sprayer system in peach production. *Plant Disease*, *104*(12), 3207–3212. https://doi.org/10.1094/PDIS-04-20-0696-RE

Bock, C. H., & Hotchkiss, M. W. (2020). A Comparison of Ground-Based Air-Blast Sprayer and Aircraft Application of Fungicides to Manage Scab in Tall Pecan Trees. *Plant Disease*, *104*(6), 1675–1684. https://doi.org/10.1094/PDIS-11-19-2345-RE

Brannen, P. (2018). *2018 GEORGIA PLANT DISEASE LOSS ESTIMATES*.

Byers, C., Virk, S., Rains, G., & Li, S. (2024). Spray deposition and uniformity assessment of unmanned aerial application systems (UAAS) at varying operational parameters.

Frontiers in Agronomy, *6*, 1418623. https://doi.org/10.3389/FAGRO.2024.1418623/BIBTEX

Cai, J., Xiong, J., Hong, Y., & Hu, R. (2021). Pesticide overuse in apple production and its socioeconomic determinants: Evidence from Shaanxi and Shandong provinces, China. *Journal of Cleaner Production*, *315*. https://doi.org/10.1016/j.jclepro.2021.128179

Carvalho, F. P. (2017). Pesticides, environment, and food safety. In *Food and Energy Security* (Vol. 6, Issue 2, pp. 48–60). Wiley-Blackwell Publishing Ltd. https://doi.org/10.1002/fes3.108

Chen, H., Lan, Y., Fritz, B. K., Clint Hoffmann, W., & Liu, S. (2021). Review of agricultural spraying technologies for plant protection using unmanned aerial vehicle (Uav). *International Journal of Agricultural and Biological Engineering*, *14*(1), 38–49. https://doi.org/10.25165/j.ijabe.20211401.5714

Chen, J., Hu, W., Dong, X., Lin, J., Gao, Z., & Qiu, B. (2024). Experimental investigation on modes of spray formation, droplet size and size distribution in a spinning disc atomizer. *Frontiers in Plant Science*, *15*, 1470745. https://doi.org/10.3389/FPLS.2024.1470745/BIBTEX

Chen, P., Douzals, J. P., Lan, Y., Cotteux, E., Delpuech, X., Pouxviel, G., & Zhan, Y. (2022). Characteristics of unmanned aerial spraying systems and related spray drift: A review. *Frontiers in Plant Science*, *13*, 870956. https://doi.org/10.3389/FPLS.2022.870956/BIBTEX

Chen, P., Lan, Y., Huang, X., Qi, H., Wang, G., Wang, J., Wang, L., & Xiao, H. (2020). Droplet deposition and control of planthoppers of different nozzles in two-stage rice with a quadrotor unmanned aerial vehicle. *Agronomy*, *10*(2). https://doi.org/10.3390/agronomy10020303

Chen, P., Ouyang, F., Wang, G., Qi, H., Xu, W., Yang, W., Zhang, Y., & Lan, Y. (2021). Droplet distributions in cotton harvest aid applications vary with the interactions among the unmanned aerial vehicle spraying parameters. *Industrial Crops and Products*, *163*. https://doi.org/10.1016/j.indcrop.2021.113324

Chen, S., Lan, Y., Zhou, Z., Ouyang, F., Wang, G., Huang, X., Deng, X., & Cheng, S. (2020). Effect of droplet size parameters on droplet deposition and drift of aerial spraying by using plant protection UAV. *Agronomy*, *10*(2). https://doi.org/10.3390/agronomy10020195

Chen, S., Yubin, L., Zhiyan, Z., & Qiuyang, L. J. and Z. (2017). Effects of spraying parameters of small plant protection UAV on droplets deposition distribution in citrus canopy. *Journal of South China Agricultural University*, *38*(5), 97–102. https://doi.org/10.7671/J.ISSN.1001-411X.2017.05.017

Chen, Y., Ozkan, H. E., Zhu, H., Derksen, R. C., & Krause, C. R. (2013). Spray deposition inside tree canopies from a newly developed variable-rate air-assisted sprayer. *Transactions of the ASABE*, *56*(6), 1263–1272. https://doi.org/10.13031/trans.56.9839

Delavarpour, N., Koparan, C., Zhang, Y., Steele, D. D., Betitame, K., Bajwa, S. G., & Sun, X. (2023). A Review of the Current Unmanned Aerial Vehicle Sprayer Applications in Precision Agriculture. *Journal of the ASABE*, *66*(3), 703–721. https://doi.org/10.13031/JA.15128

DJI. (2022). *Unmanned Aircraft Flight Manual*. https://www.dji.com/t20p/downloads

Durham, T. C., & Mizik, T. (2021). Comparative Economics of Conventional, Organic, and Alternative Agricultural Production Systems. *Economies 2021, Vol. 9, Page 64*, *9*(2), 64. https://doi.org/10.3390/ECONOMIES9020064

EPA. (2024). *Types of Pesticide Ingredients | US EPA*. https://www.epa.gov/ingredients-used-pesticide-products/types-pesticide-ingredients

EPA. (2025). *Food and Pesticides | US EPA*. https://www.epa.gov/safepestcontrol/food-and-pesticides

FAOSTAT. (2023). https://www.fao.org/faostat/en/#compare

FAOSTAT. (2025). https://www.fao.org/faostat/en/#data

FAOSTAT, F. and A. O. of the U. N. (2022). *Pesticides use and trade*. http://www.fao.org/faostat/en/#data/RP.

Fruit, Tree Nut, and Berry Production. (2017). www.nass.usda.gov/AgCensus

Gao, Q., Ma, J., Liu, Q., Liao, M., Xiao, J., Jiang, M., Shi, Y., & Cao, H. (2020). Effect of application method and formulation on prothioconazole residue behavior and mycotoxin contamination in wheat. *Science of the Total Environment*, *729*. https://doi.org/10.1016/j.scitotenv.2020.139019

García-Munguía, A., Guerra-Ávila, P. L., Islas-Ojeda, E., Flores-Sánchez, J. L., Vázquez-Martínez, O., García-Munguía, A. M., & García-Munguía, O. (2024a). A Review of Drone Technology and Operation Processes in Agricultural Crop Spraying. In *Drones* (Vol. 8, Issue 11). Multidisciplinary Digital Publishing Institute (MDPI). https://doi.org/10.3390/drones8110674

García-Munguía, A., Guerra-Ávila, P. L., Islas-Ojeda, E., Flores-Sánchez, J. L., Vázquez-Martínez, O., García-Munguía, A. M., & García-Munguía, O. (2024b). A Review of Drone Technology and Operation Processes in Agricultural Crop Spraying. In *Drones* (Vol. 8, Issue 11). Multidisciplinary Digital Publishing Institute (MDPI). https://doi.org/10.3390/drones8110674

Ghafoor, A., Khan, F. A., Khorsandi, F., Khan, M. A., Nauman, H. M., & Farid, M. U. (2022). Development and Evaluation of a Prototype Self-Propelled Crop Sprayer for Agricultural Sustainability in Small Farms. *Sustainability 2022, Vol. 14, Page 9204*, *14*(15), 9204. https://doi.org/10.3390/SU14159204

Gill, M. (2024). *AccuStain Software User Guide*.

Guo, Q., Zhu, Y., Tang, Y., Hou, C., He, Y., Zhuang, J., Zheng, Y., & Luo, S. (2020). CFD simulation and experimental verification of the spatial and temporal distributions of the downwash airflow of a quad-rotor agricultural UAV in hover. *Computers and Electronics in Agriculture*, *172*, 105343. https://doi.org/10.1016/J.COMPAG.2020.105343

Guo, S., Li, J., Yao, W., Zhan, Y., Li, Y., & Shi, Y. (2019). Distribution characteristics on droplet deposition of wind field vortex formed by multi-rotor UAV. *PLoS ONE*, *14*(7). https://doi.org/10.1371/journal.pone.0220024

Guo, S., Yao, W., Xu, T., Ma, H., Sun, M., Chen, C., & Lan, Y. (2022). Assessing the application of spot spray in Nanguo pear orchards: Effect of nozzle type, spray volume rate and adjuvant. *Pest Management Science*, *78*(8), 3564–3575. https://doi.org/10.1002/ps.6999

Hanna, M., Kruckeberg, J., Darr, M., & Steward, B. (2009). *Nozzle and droplet size effects on pesticide performance and drift*.

Hoying, S. A. (2017). Orchard Crops. *Encyclopedia of Applied Plant Sciences*, *3*, 246–254. https://doi.org/10.1016/B978-0-12-394807-6.00003-4

Hu, Y., Yang, H., Hou, B., Xi, Z., & Yang, Z. (2022). Influence of Spray Control Parameters on the Performance of an Air-Blast Sprayer. *Agriculture (Switzerland)*, *12*(8). https://doi.org/10.3390/agriculture12081260

Huang, K. M., Guan, Z., & Hammami, A. M. (2022). The U.S. Fresh Fruit and Vegetable Industry: An Overview of Production and Trade. *Agriculture (Switzerland)*, *12*(10). https://doi.org/10.3390/agriculture12101719

Hüesker, F., & Lepenies, R. (2022). Why does pesticide pollution in water persist? *Environmental Science and Policy*, *128*, 185–193. https://doi.org/10.1016/j.envsci.2021.11.016

Jacto Inc. (2011). *Operator's Manual*. www.jacto.com

Jiang, Y., He, X., Song, J., Liu, Y., Wang, C., Li, T., Qi, P., Yu, C., & Chen, F. (2022). Comprehensive assessment of intelligent unmanned vehicle techniques in pesticide application: A case study in pear orchard. *Frontiers in Plant Science*, *13*. https://doi.org/10.3389/fpls.2022.959429

Kumhar, K., Jat, R. D., Author, C., Chand Kumhar, K., Singh Beniwal, B., Dhan Jat, R., Patel, B., Kumar, A., Raj, H., Kumar, M., Kumar, N., & Kumar, S. (2022). Plant Disease Management Approaches for Organic Crop Production in Indian Scenario: A Critical Review Journal of Plant Bioinformatics and Biotechnology Plant Disease Management Approaches for Organic Crop Production in Indian Scenario: A Critical Review Plant Disease Management Approaches for Organic Crop Production in Indian Scenario: A Critical Review. *J. Plant Bioinform. Biotechnol*, *2*(1), 1–12. https://doi.org/10.22034/jpbb.2022.327017.1018

Kuosmanen, N., Yli-Heikkilä, M., Väre, M., & Kuosmanen, T. (2021). Productive performance of organic crop farms in Finland 2010–2017. *Organic Agriculture*, *11*(3), 379–392. https://doi.org/10.1007/S13165-020-00343-X/TABLES/3

Li, X., Giles, D. K., Niederholzer, F. J., Andaloro, J. T., Lang, E. B., & Watson, L. J. (2021). Evaluation of an unmanned aerial vehicle as a new method of pesticide application for almond crop protection. *Pest Management Science*, *77*(1), 527–537. https://doi.org/10.1002/ps.6052

Lopes, L. de L., Cunha, J. P. A. R. da, & Nomelini, Q. S. S. (2023). Use of Unmanned Aerial Vehicle for Pesticide Application in Soybean Crop. *AgriEngineering 2023, Vol. 5, Pages 2049-2063*, *5*(4), 2049–2063. https://doi.org/10.3390/AGRIENGINEERING5040126

Luo, C. X., Schnabel, G., Hu, M., & De Cal, A. (2022). Global distribution and management of peach diseases. In *Phytopathology Research* (Vol. 4, Issue 1). BioMed Central Ltd. https://doi.org/10.1186/s42483-022-00134-0

Maggi, F., Tang, F. H. M., & Tubiello, F. N. (2023). Agricultural pesticide land budget and river discharge to oceans. *Nature*, *620*(7976), 1013–1017. https://doi.org/10.1038/s41586-023-06296-x

Mahmud, M. S., He, L., Heinemann, P., Choi, D., & Zhu, H. (2023). Unmanned aerial vehicle based tree canopy characteristics measurement for precision spray applications. *Smart Agricultural Technology*, *4*, 100153. https://doi.org/10.1016/J.ATECH.2022.100153

Mahmud, M. S., Zahid, A., He, L., & Martin, P. (2021). Opportunities and possibilities of developing an advanced precision spraying system for tree fruits. In *Sensors* (Vol. 21, Issue 9). MDPI AG. https://doi.org/10.3390/s21093262

Manganaris, G. A., Minas, I., Cirilli, M., Torres, R., Bassi, D., & Costa, G. (2022). Peach for the future: A specialty crop revisited. *Scientia Horticulturae*, *305*. https://doi.org/10.1016/j.scienta.2022.111390

Martinez-Guanter, J., Agüera, P., Agüera, J., & Pérez-Ruiz, M. (2020). Spray and economics assessment of a UAV-based ultra-low-volume application in olive and citrus orchards. *Precision Agriculture*, *21*(1), 226–243. https://doi.org/10.1007/s11119-019-09665-7

Meng, Y., Su, J., Song, J., Chen, W. H., & Lan, Y. (2020). Experimental evaluation of UAV spraying for peach trees of different shapes: Effects of operational parameters on droplet distribution. *Computers and Electronics in Agriculture*, *170*. https://doi.org/10.1016/j.compag.2020.105282

Miguez, M., Deleón, R., Vicente, G., & Zoppolo, R. (2019). Real time tree row volume estimation for efficient application of phytosanitary products in fruit trees. *Proceedings - IEEE International Symposium on Circuits and Systems*, *2019-May*. https://doi.org/10.1109/ISCAS.2019.8702561

Mogili, U. R., & Deepak, B. B. V. L. (2018). Review on Application of Drone Systems in Precision Agriculture. *Procedia Computer Science*, *133*, 502–509. https://doi.org/10.1016/J.PROCS.2018.07.063

Mohanty, S. P., & Raheman, H. (2024). Performance optimization of an air-assisted electrostatic spraying unit using response surface methodology. *Journal of Electrostatics*, *131*, 103963. https://doi.org/10.1016/J.ELSTAT.2024.103963

Mohsan, S. A. H., Othman, N. Q. H., Li, Y., Alsharif, M. H., & Khan, M. A. (2023). Unmanned aerial vehicles (UAVs): practical aspects, applications, open challenges, security issues, and future trends. *Intelligent Service Robotics 2023 16:1*, *16*(1), 109–137. https://doi.org/10.1007/S11370-022-00452-4

Muhammad, M. N., Wayayok, A., Mohamed Shariff, A. R., Abdullah, A. F., & Husin, E. M. (2019). Droplet deposition density of organic liquid fertilizer at low altitude UAV aerial spraying in rice cultivation. *Computers and Electronics in Agriculture*, *167*. https://doi.org/10.1016/j.compag.2019.105045

Muthuri, C. W., Kuyah, S., Njenga, M., Kuria, A., Öborn, I., & van Noordwijk, M. (2023). Agroforestry's contribution to livelihoods and carbon sequestration in East Africa: A systematic review. *Trees, Forests and People*, *14*, 100432. https://doi.org/10.1016/J.TFP.2023.100432

Nan, Y., Zhang, H., Zheng, J., Yang, K., & Ge, Y. (2023). Low-volume precision spray for plant pest control using profile variable rate spraying and ultrasonic detection. *Frontiers in Plant Science*, *13*. https://doi.org/10.3389/fpls.2022.1042769

Nogueira Martins, R., Marcus Fialho Moraes, H., Alexandre Moreira de Freitas, M., da Costa Lima, A., & Ribeiro Furtado Junior, M. (2021). *Effect of nozzle type and pressure on spray droplet characteristics*.

Nuyttens, D., Baetens, K., De Schampheleire, M., & Sonck, B. (2007). Effect of nozzle type, size and pressure on spray droplet characteristics. *Biosystems Engineering*, *97*(3), 333–345. https://doi.org/10.1016/j.biosystemseng.2007.03.001

Ozkan, E. (2024). *Drones for Spraying Pesticides - Opportunities and Challenges*. https://ohioline.osu.edu/factsheet/fabe-540

Paul, R. A. I., Palanisamy, M. A., Peramaiyan, P., Kumar, V., Bagavathiannan, M., Gurjar, B., Vijayakumar, S., Djanaguiraman, M., Pazhanivelan, S., & Ramasamy, K. (2024). Spray volume optimization with UAV-based herbicide application for effective droplet deposition and weed control in direct-seeded rice. *Frontiers in Agronomy*, *6*, 1491842. https://doi.org/10.3389/FAGRO.2024.1491842/BIBTEX

Perez, A., Ferreira, G., & Minor, T. (2017). *Fruit and Tree Nuts Outlook*.

Privitera, S., Manetto, G., Pascuzzi, S., Pessina, D., & Cerruto, E. (2023). Drop Size Measurement Techniques for Agricultural Sprays:A State-of-The-Art Review. In *Agronomy* (Vol. 13, Issue 3). MDPI. https://doi.org/10.3390/agronomy13030678

Protzman, E. (2023). *Peaches and Nectarines: Global Growth in Production Slowing While Exports Plateau*.

Qin, W., Xue, X., Zhang, S., Gu, W., & Wang, B. (2018). Droplet deposition and efficiency of fungicides sprayed with small UAV against wheat powdery mildew. *International Journal of Agricultural and Biological Engineering*, *11*(2), 27–32. https://doi.org/10.25165/j.ijabe.20181102.3157

Raj, M., N B, H., Gupta, S., Atiquzzaman, M., Rawlley, O., & Goel, L. (2024). Leveraging precision agriculture techniques using UAVs and emerging disruptive technologies. In *Energy Nexus* (Vol. 14). Elsevier Ltd. https://doi.org/10.1016/j.nexus.2024.100300

Ritchie, H., Rosado, P., & Roser, M. (2023). Agricultural Production. *Our World in Data*. https://ourworldindata.org/agricultural-production

Sahni, R. K., Kumar, S. P., Thorat, D., Rajwade, Y., Jyoti, B., Ranjan, J., & Anand, R. (2024). Drone Spraying System for Efficient Agrochemical Application in Precision Agriculture. *Applications of Computer Vision and Drone Technology in Agriculture 4.0*, 225–244. https://doi.org/10.1007/978-981-99-8684-2_13

Santosa, E., Susila, A. D., Widodo, W. D., Nasrullah, N., Ruwaida, I. P., & Sari, R. (2021). Exploring fruit tree species as multifunctional greenery: A case of its distribution in indonesian cities. *Sustainability (Switzerland)*, *13*(14), 7835. https://doi.org/10.3390/SU13147835/S1

Sassu, A., Psiroukis, V., Bettucci, F., Ghiani, L., Fountas, S., & Gambella, F. (2024). Unmanned aerial system plant protection products spraying performance evaluation on a vineyard. *Precision Agriculture*, *25*(4), 2082–2112. https://doi.org/10.1007/s11119-024-10155-8

Schick, R. J. (2008). *Spray Technology Reference Guide: Understanding Drop Size*.

Schnabel, D. G., & Brannen, D. P. M. (2022). Biology, epidemiology, and management of diseases of peach driving the spray program in the southeastern United States. *Scientia Horticulturae*, *295*. https://doi.org/10.1016/j.scienta.2021.110818

Schreinemachers, P., Grovermann, C., Praneetvatakul, S., Heng, P., Nguyen, T. T. L., Buntong, B., Le, N. T., & Pinn, T. (2020). How much is too much? Quantifying pesticide overuse in vegetable production in Southeast Asia. *Journal of Cleaner Production*, *244*. https://doi.org/10.1016/j.jclepro.2019.118738

Shan, C., Wang, G., Wang, H., Xie, Y., Wang, H., Wang, S., Chen, S., & Lan, Y. (2021). Effects of droplet size and spray volume parameters on droplet deposition of wheat herbicide application by using UAV. *International Journal of Agricultural and Biological Engineering*, *14*(1), 74–81. https://doi.org/10.25165/IJABE.V14I1.6129

Shan, C., Xue, C., Zhang, L., Song, C., Kaousar, R., Wang, G., & Lan, Y. (2024a). Effects of different spray parameters of plant protection UAV on the deposition characteristics of droplets in apple trees. *Crop Protection*, *184*. https://doi.org/10.1016/j.cropro.2024.106835

Shan, C., Xue, C., Zhang, L., Song, C., Kaousar, R., Wang, G., & Lan, Y. (2024b). Effects of different spray parameters of plant protection UAV on the deposition characteristics of droplets in apple trees. *Crop Protection*, *184*. https://doi.org/10.1016/j.cropro.2024.106835

Sharma, A., Kumar, V., Shahzad, B., Tanveer, M., Sidhu, G. P. S., Handa, N., Kohli, S. K., Yadav, P., Bali, A. S., Parihar, R. D., Dar, O. I., Singh, K., Jasrotia, S., Bakshi, P., Ramakrishnan, M., Kumar, S., Bhardwaj, R., & Thukral, A. K. (2019). Worldwide pesticide usage and its impacts on ecosystem. *SN Applied Sciences*, *1*(11), 1–16. https://doi.org/10.1007/S42452-019-1485-1/TABLES/4

Silva, J. E., da Silva, W. H. B., Ferraz, M. A. J., Menezes, E. A. S., da Costa, O. P., Inácio, F. D., Barboza, T. O. C., Melo, C. A. D., Carvalho, G. R., & Santos, A. F. dos. (2024). Impact of spray volume and flight speed on the efficiency of drone applications in coffee plants of different ages. *Smart Agricultural Technology*, *9*, 100694. https://doi.org/10.1016/J.ATECH.2024.100694

Song, Y., Huang, Q., Huang, G., Liu, M., Cao, L., Li, F., Zhao, P., & Cao, C. (2022). The Effects of Adjuvants on the Wetting and Deposition of Insecticide Solutions on Hydrophobic Wheat Leaves. *Agronomy*, *12*(9). https://doi.org/10.3390/agronomy12092148

Sookhtanlou, M., Allahyari, M. S., & Surujlal, J. (2022). Health Risk of Potato Farmers Exposed to Overuse of Chemical Pesticides in Iran. *Safety and Health at Work*, *13*(1), 23–31. https://doi.org/10.1016/j.shaw.2021.09.004

Srinivasarao, A., Khura, T. K., Parray, R. A., Kushwaha, H. L., & Mani, I. (2021). Spray droplet deposition, collection, and analysis techniques: A review. *~ 156 ~ The Pharma Innovation Journal*, *6*, 156–165. http://www.thepharmajournal.com

Tang, Y., Fu, Y., Guo, Q., Huang, H., Tan, Z., & Luo, S. (2023). Numerical simulation of the spatial and temporal distributions of the downwash airflow and spray field of a co-axial eight-rotor plant protection UAV in hover. *Computers and Electronics in Agriculture*, *206*, 107634. https://doi.org/10.1016/J.COMPAG.2023.107634

Tang, Y., Hou, C. J., Luo, S. M., Lin, J. T., Yang, Z., & Huang, W. F. (2018). Effects of operation height and tree shape on droplet deposition in citrus trees using an unmanned aerial vehicle. *Computers and Electronics in Agriculture*, *148*, 1–7. https://doi.org/10.1016/j.compag.2018.02.026

Thomine, E., Mumford, J., Rusch, A., & Desneux, N. (2022). Using crop diversity to lower pesticide use: Socio-ecological approaches. In *Science of the Total Environment* (Vol. 804). Elsevier B.V. https://doi.org/10.1016/j.scitotenv.2021.150156

Tsouros, D. C., Bibi, S., & Sarigiannidis, P. G. (2019). A review on UAV-based applications for precision agriculture. In *Information (Switzerland)* (Vol. 10, Issue 11). MDPI AG. https://doi.org/10.3390/info10110349

Tudi, M., Ruan, H. D., Wang, L., Lyu, J., Sadler, R., Connell, D., Chu, C., & Phung, D. T. (2021). Agriculture development, pesticide application and its impact on the environment. In *International Journal of Environmental Research and Public Health* (Vol. 18, Issue 3, pp. 1–24). MDPI AG. https://doi.org/10.3390/ijerph18031112

USDA. (2022). *Fruit, Tree Nut, and Berry Production*. www.nass.usda.gov/AgCensus

USDA. (2023). *USDA - Production - Peaches & Nectarines*. https://www.fas.usda.gov/data/production/commodity/0579309

USDA. (2024). *2022 Census of Agriculture*.

van der Merwe, D., Burchfield, D. R., Witt, T. D., Price, K. P., & Sharda, A. (2020). Drones in agriculture. In *Advances in Agronomy* (Vol. 162, pp. 1–30). Academic Press Inc. https://doi.org/10.1016/bs.agron.2020.03.001

van Veelen, M. J., Roveri, G., Voegele, A., Cappello, T. D., Masè, M., Falla, M., Regli, I. B., Mejia-Aguilar, A., Mayrgündter, S., & Strapazzon, G. (2023). Drones reduce the treatment-free interval in search and rescue operations with telemedical support – A randomized controlled trial. *The American Journal of Emergency Medicine*, *66*, 40–44. https://doi.org/10.1016/J.AJEM.2023.01.020

Wandkar, S. V., Bhatt, Y. C., Jain, H. K., Nalawade, S. M., & Pawar, S. G. (2018). Real-Time Variable Rate Spraying in Orchards and Vineyards: A Review. In *Journal of The Institution of Engineers (India): Series A* (Vol. 99, Issue 2, pp. 385–390). Springer India. https://doi.org/10.1007/s40030-018-0289-4

Wang, G., Lan, Y., Qi, H., Chen, P., Hewitt, A., & Han, Y. (2019). Field evaluation of an unmanned aerial vehicle (UAV) sprayer: effect of spray volume on deposition and the control of pests and disease in wheat. *Pest Management Science*, *75*(6), 1546–1555. https://doi.org/10.1002/ps.5321

Wang, G., Lan, Y., Yuan, H., Qi, H., Chen, P., Ouyang, F., & Han, Y. (2019). Comparison of Spray Deposition, Control Efficacy on Wheat Aphids and Working Efficiency in the Wheat Field of the Unmanned Aerial Vehicle with Boom Sprayer and Two Conventional Knapsack Sprayers. *Applied Sciences 2019, Vol. 9, Page 218*, *9*(2), 218. https://doi.org/10.3390/APP9020218

Wang, J., Lan, Y., Zhang, H., Zhang, Y., Wen, S., Yao, W., & Deng, J. (2018). Drift and deposition of pesticide applied by UAV on pineapple plants under different meteorological conditions. *International Journal of Agricultural and Biological Engineering*, *11*(6), 5–12. https://doi.org/10.25165/IJABE.V11I6.4038

Wei, Z., Li, R., Xue, X., Sun, Y., Zhang, S., Li, Q., Chang, C., Zhang, Z., Sun, Y., & Dou, Q. (2023). Research Status, Methods and Prospects of Air-Assisted Spray Technology. In *Agronomy* (Vol. 13, Issue 5). MDPI. https://doi.org/10.3390/agronomy13051407

Wei, Z., Xue, X., Salcedo, R., Zhang, Z., Gil, E., Sun, Y., Li, Q., Shen, J., He, Q., Dou, Q., & Zhang, Y. (2023). Key Technologies for an Orchard Variable-Rate Sprayer: Current Status and Future Prospects. In *Agronomy* (Vol. 13, Issue 1). MDPI. https://doi.org/10.3390/agronomy13010059

Wu, W. Te, Chen, J. M., Chang, Y. Y., Lin, S. Da, Chen, S. T., & Hung, Y. T. (2024). Assessing the effectiveness of mitigating pesticide-related disease risk among pesticide-spraying drone operators in Taiwan. *American Journal of Industrial Medicine*, *67*(2), 110–118. https://doi.org/10.1002/AJIM.23551

Yan, Y., Lan, Y., Wang, G., Hussain, M., Wang, H., Yu, X., Shan, C., Wang, B., & Song, C. (2023). Evaluation of the deposition and distribution of spray droplets in citrus orchards by plant protection drones. *Frontiers in Plant Science*, *14*. https://doi.org/10.3389/fpls.2023.1303669

Zhan, Y., Chen, P., Xu, W., Chen, S., Han, Y., Lan, Y., & Wang, G. (2022). Influence of the downwash airflow distribution characteristics of a plant protection UAV on spray deposit distribution. *Biosystems Engineering*, *216*, 32–45. https://doi.org/10.1016/J.BIOSYSTEMSENG.2022.01.016

Zhao, Q., Pan, Y., & Xia, X. (2020). *Internet can do help in the reduction of pesticide use by farmers: evidence from rural China*. https://doi.org/10.1007/s11356-020-10576-8/Published

Zhu, H., Salyani, M., & Fox, R. D. (2011). A portable scanning system for evaluation of spray deposit distribution. *Computers and Electronics in Agriculture*, *76*(1), 38–43. https://doi.org/10.1016/J.COMPAG.2011.01.003